The Statistical Hadronization Model: successes and some open issues

- thermal particle production – from 1951 till now
- the statistical hadronization model, SHM for (u,d,s) hadrons and light nuclei
- focus: production of loosely bound states
- outlook

pbm

66 Cracow School of Theoretical Physics

Krakow, June 15 – 19, 2026

see also for more historical context and detailed references:

The quark-gluon plasma: diagnosis with thermal hadron production from the early history until detailed characterization at high energy colliders

Peter Braun-Munzinger, Krzysztof Redlich, Johanna Stachel (Jun 5, 2025)

e-Print: 2506.04733 [nucl-th]

Happy 90. Birthday
and all the best for
many good years to come!

long time collaborators: Krzysztof Redlich, Anton Andronic, Johanna Stachel

thermal particle production - the very early days: Pomeranchuk 1951, Fermi 1953, Landau 1953, Hagedorn 1965, Bjorken & Brodsky 1970, Shuryak 1978

QCD 1973 Gross, Wilczek, Politzer

thermal particle production: 1st quantitative steps – Hagedorn's limiting temperature

QCD and QGP, Collins and Perry 1974

Cabibbo and Parisi 1975 1st phase diagram Phys. Lett. 59B (1975) 76

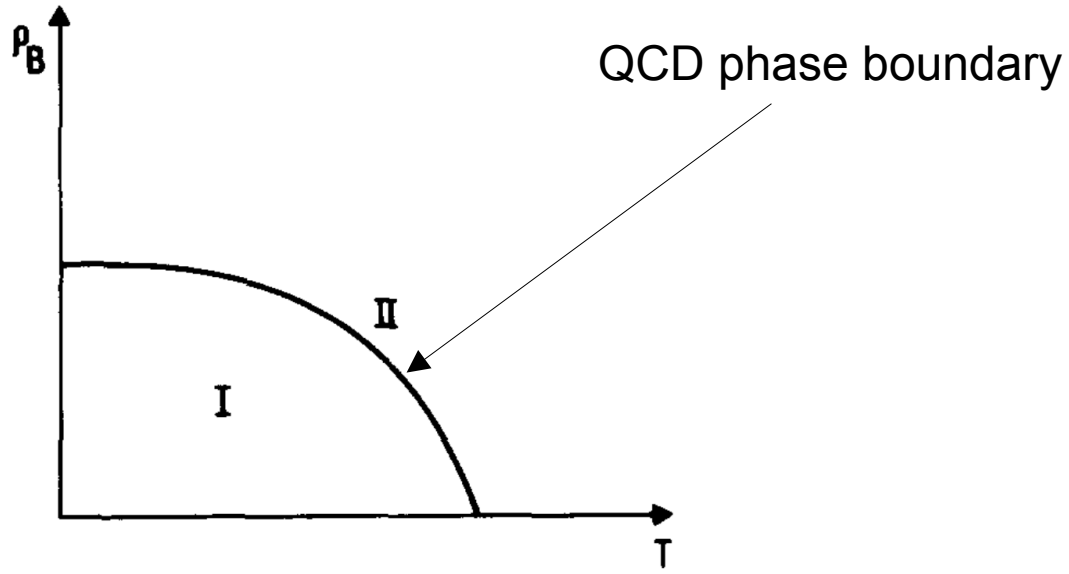

Fig. 1. Schematic phase diagram of hadronic matter. ρ_B is the density of baryonic number. Quarks are confined in phase I and unconfined in phase II.

development of ideas for thermal particle production

- Hagedorn and Rafelski 1980 hot hadronic matter and nuclear collisions, Phys. Lett. B97 (1980) 136
- Hagedorn and Redlich 1985 statistical thermodynamics – canonical or grand canonical?, Z. Physik C87 (1985) 541
- Satz and Cleymans, 1993 thermal hadron production in high energy heavy ion collisions, Z. Physik C57 (1993) 135
- Braun-Munzinger, Stachel, Wessels, Xu, thermal equilibrium and expansion in nucleus-nucleus collisions at the AGS, Phys. Lett. B 344 (1995) 43
- Braun-Munzinger, Stachel, Wessels, Xu, thermal and hadrochemical equilibration in nucleus-nucleus collisions at the SPS, Phys. Lett. B365 (1996) 1
- Becattini, Z. Phys. C 69 (1996) 3, 485-492

pbm, J. Stachel, J.P. Wessels, Nu Xu

1st successful description of experimental particle yields, 1994
Phys. Lett.B 344 (1995) 43-48, nucl-th/9410026 [nucl-th]

1st phase diagram with data, 1995
Phys.Lett. B 365 (1996) 1-6, nucl-th/9508020 [nucl-th]

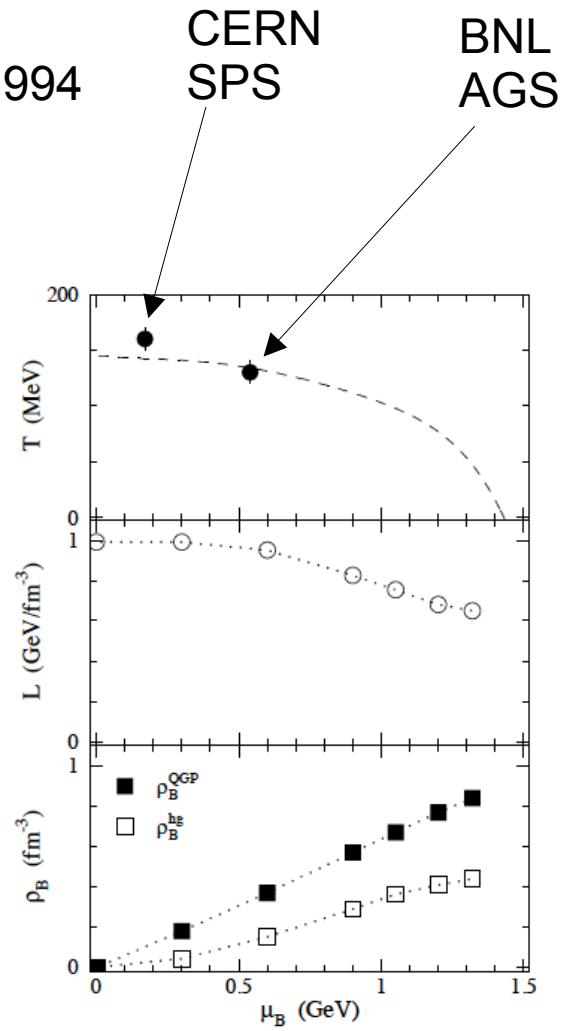

for central collisions of 14.6 A GeV/c Si + Au(Pb).

Particles	Thermal Model		Data	
	T=.120 GeV	T=.140 GeV	exp. ratio	rapidity
$\pi/(p+n)$	1.29	1.34	1.05(5)	0.6 - 2.8
$d/(p+n)$	$4.3 \cdot 10^{-2}$	$5.8 \cdot 10^{-2}$	$3.0(3) \cdot 10^{-2}$	0.4 - 1.6
$\bar{p}/p$	$1.47 \cdot 10^{-4}$	$5.8 \cdot 10^{-4}$	$4.5(5) \cdot 10^{-4}$	0.8 - 2.2
K^+/π^+	0.23	0.27	0.19(2)	0.6 - 2.2
K^-/π^-	$5.0 \cdot 10^{-2}$	$6.2 \cdot 10^{-2}$	$3.5(5) \cdot 10^{-2}$	0.6 - 2.3
K_s^0/π^+	0.14	0.16	$9.7(15) \cdot 10^{-2}$	2.0 - 3.5
K^+/K^-	4.6	4.3	4.4(4)	0.7 - 2.3
$\Lambda/(p+n)$	$9.5 \cdot 10^{-2}$	0.11	$8.0(16) \cdot 10^{-2}$	1.4 - 2.9
$\bar{\Lambda}/\Lambda$	$8.8 \cdot 10^{-4}$	$3.7 \cdot 10^{-3}$	$2.0(8) \cdot 10^{-3}$	1.2 - 1.7
$\phi/(K^+ + K^-)$	$2.4 \cdot 10^{-2}$	$3.6 \cdot 10^{-2}$	$1.34(36) \cdot 10^{-2}$	1.2 - 2.0
Ξ^-/Λ	$6.4 \cdot 10^{-2}$	$7.2 \cdot 10^{-2}$	0.12(2)	1.4 - 2.9
$\bar{d}/\bar{p}$	$1.1 \cdot 10^{-5}$	$4.7 \cdot 10^{-5}$	$1.0(5) \cdot 10^{-5}$	2.0

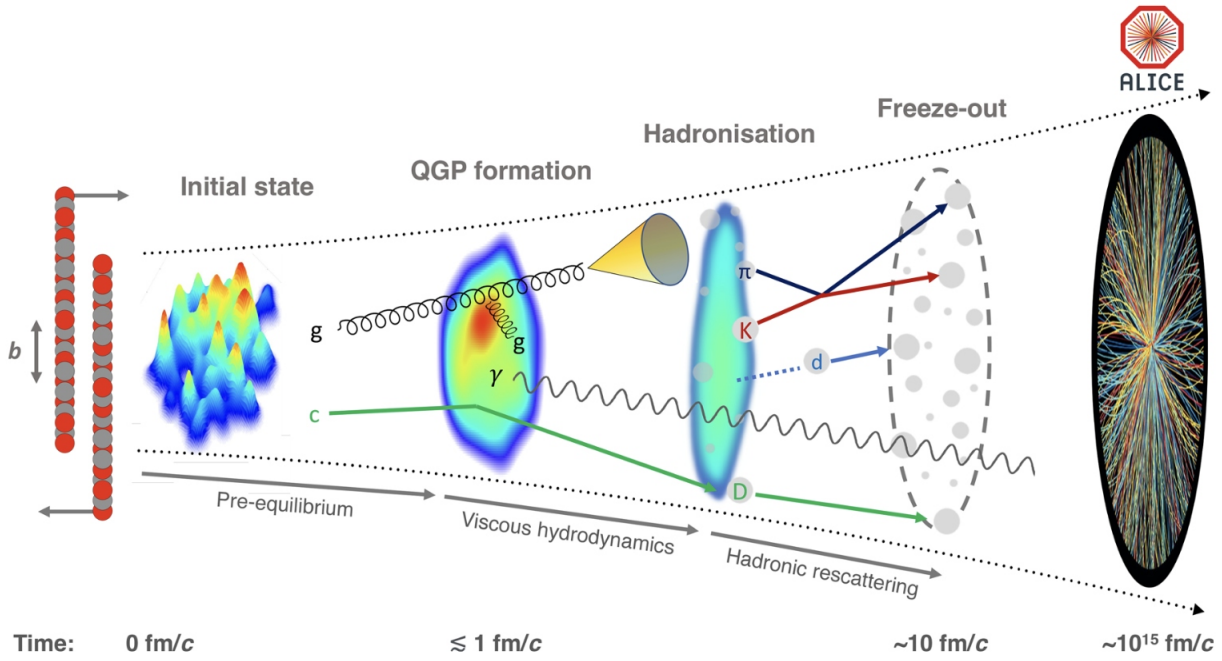

The evolution of a heavy-ion collision at LHC energies

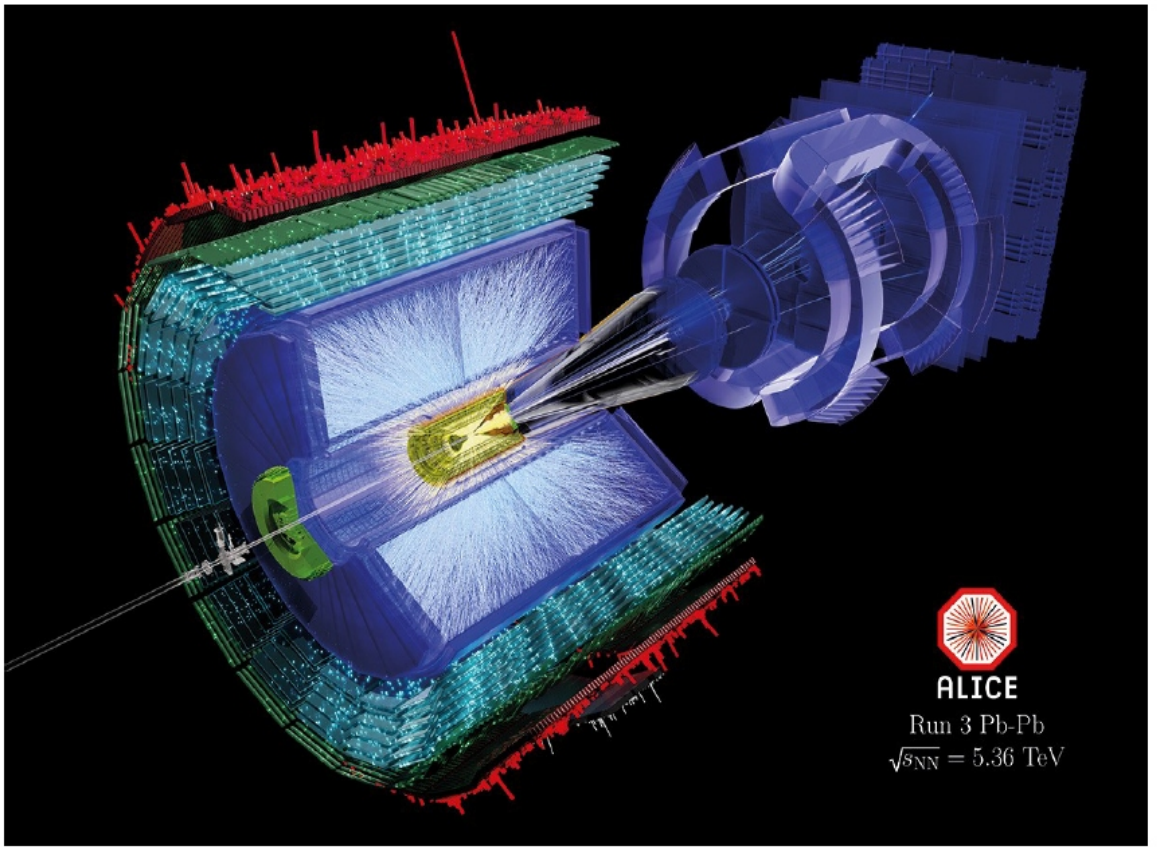

ALICE in 2023 Run 3

Particle production at the QCD phase boundary

Production of hadrons and (anti-)nuclei at LHC

at LHC energy, μ_B = 0.71 +/– 0.45 MeV

PRL 133 (2024) 9,092301

1 free parameter: temperature T

T = 156.5 ± 1.5 MeV

agreement over 9 orders of magnitude with QCD statistical operator prediction (- strong decays need to be added)

A. Andronic, P. Braun-Munzinger, K. Redlich, J. Stachel, Nature 561 (2018) 321

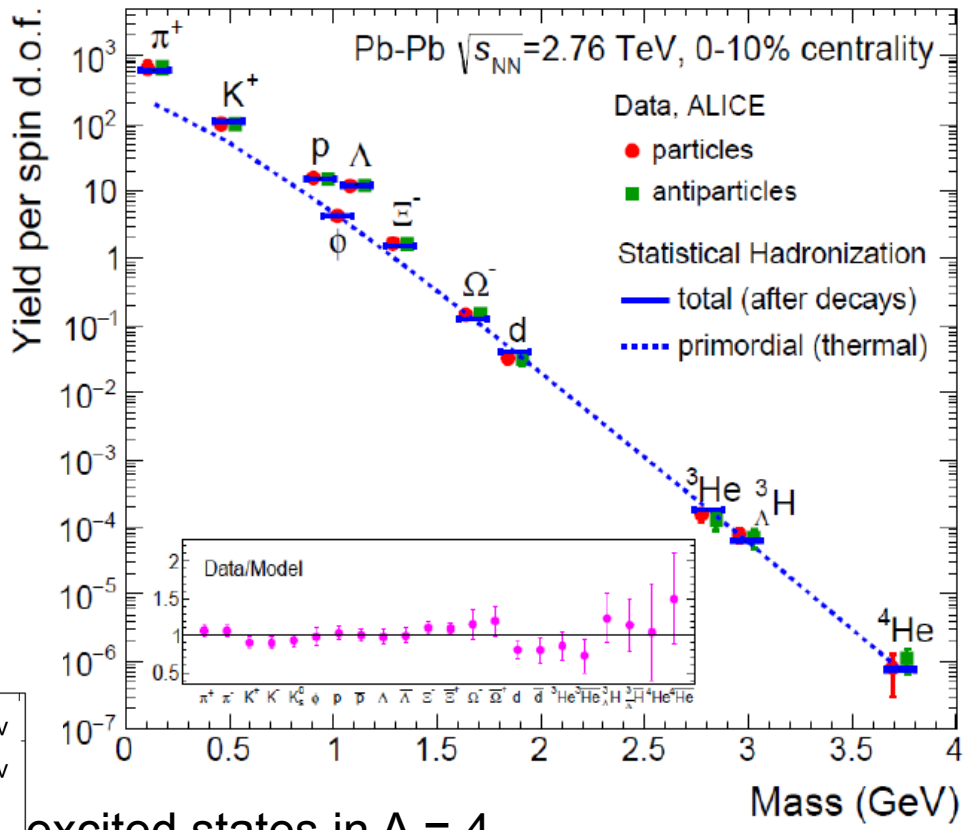

- matter and antimatter are formed in equal portions at LHC
- even large very fragile hypernuclei follow the same systematics

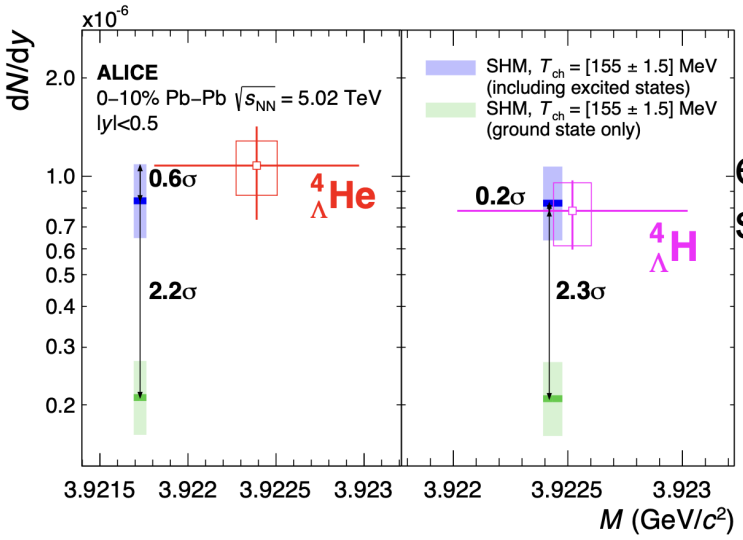

Phys.Rev.Lett. 134 (2025) 16, 162301

excited states in A = 4 systems matter

at LHC energy, all chemical potentials vanish, so strangeness is immaterial for particle production, particle yields ~ $M^{3/2}$ exp(-M/T) for large systems (no 'strangeness enhancement')

QCD phase diagram from 'statistical hadronization model'

update 2025

T_{pc} = 156.5 MeV

hadronic matter cannot be heated to T > T_{CF} even at LHC energy

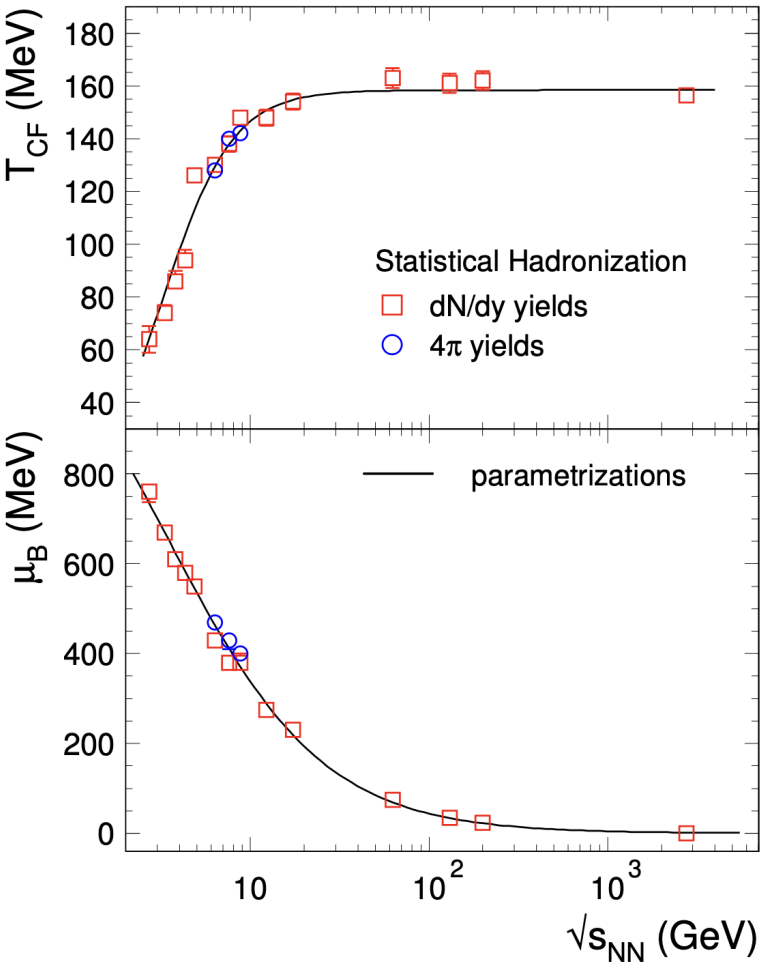

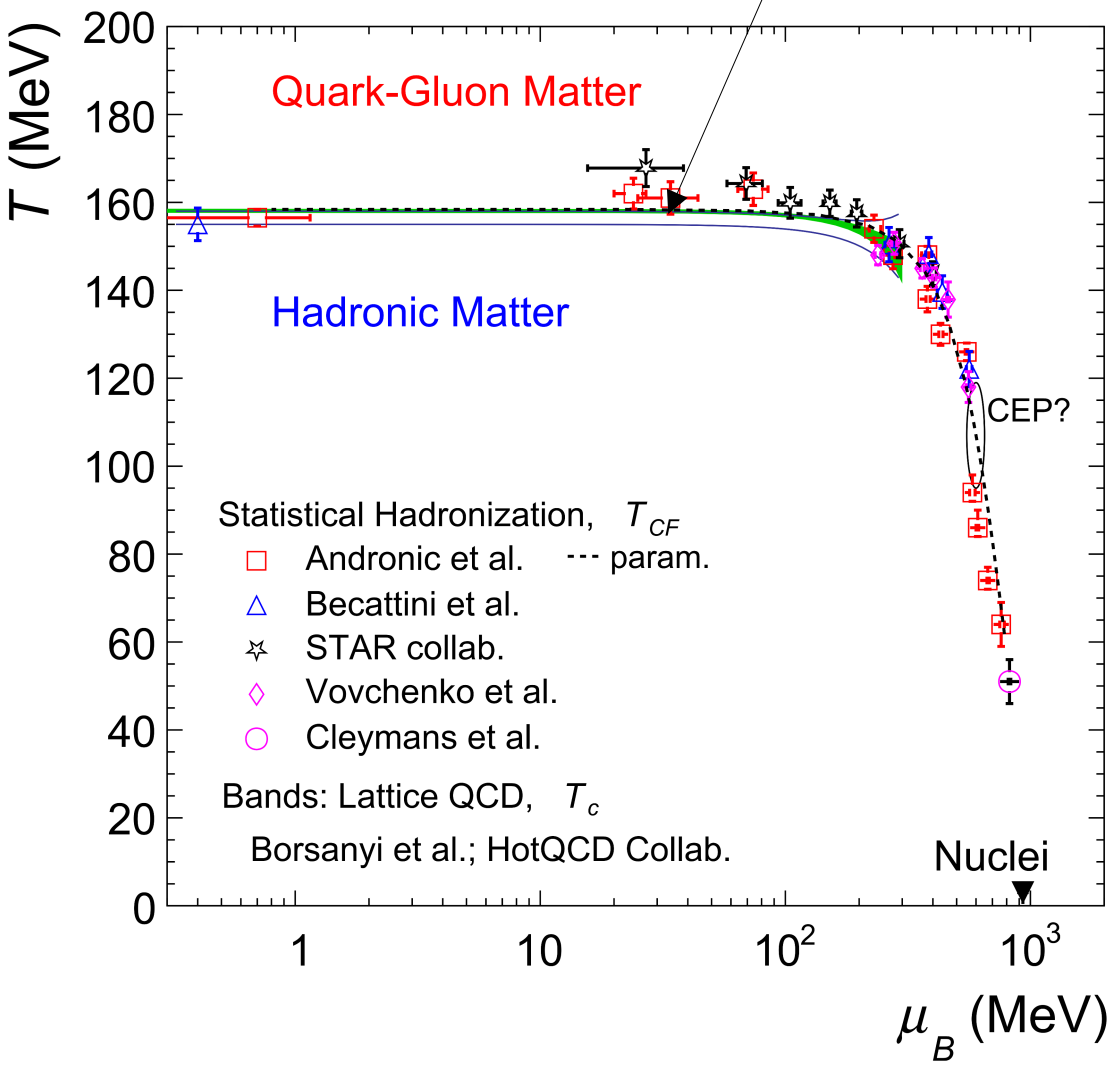

lattice predictions in quantitative agreement with results from statistical hadronization model,

CEP from Phys. Rev.D 111 (2025) 3, L031502

SHM and higher moments

SHM should work not only for 1st moment but for all higher moments as well

for application to net baryon fluctuations, see recent review

2601.18666 [nucl-ex], pbm, Anar Rustamov, Nu Xu,

The phase structure of QCD: Fluctuations and Correlations

to appear in Ann. Rev. Nucl. Part. Phys. 2027

see also: **pbm, B. Friman, K. Redlich, A. Rustamov, J. Stachel**

Nucl. Phys. A 1008 (2021) 122141 2007.02463 [nucl-th]

teaser: does heavy charmonium fit into this picture?

A.Andronic et al., PLB 797 (2019) 134836

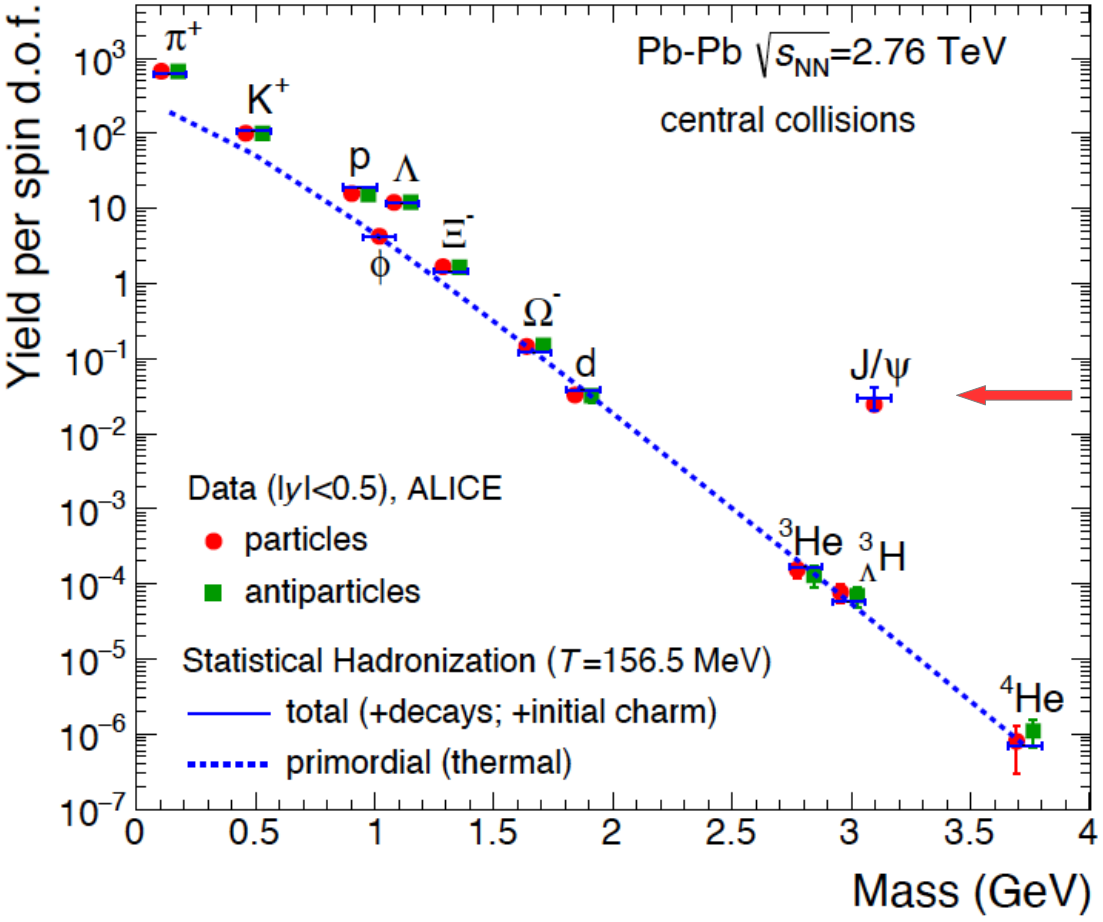

yes, but what about this factor of 900?

observed strong enhancement: clear sign for deconfinement of charm quarks, see Johanna's talk on Friday

see also the very recent review 2606.14799 [nucl-ex] by Andronic, pbm, Redlich, Stachel

Conclusion of European Strategy Meeting, June 2025, Venice

slide: courtesy of Urs Wiedemann, CERN

Quantitative support for a default picture of AA

$\tau_{dec.} \approx 10$ fm/c
$V_{dec.} \approx 5000$ fm^3
$\varepsilon(\tau_{dec.}) \approx 0.4$ GeV/fm^3

$T_{kin.} \approx 100 - 150$ MeV
$v_{T,kin.} \approx 0.65\ c$
$\tau_{hadr.} \approx 1 -$ few fm/c

$T_{chem.} = 156 \pm 2$ MeV

η/s at $T_c \approx 0.06 - 0.12$
$2\pi T D_s$ at $T_c \approx 1.5 - 4.5$
$T_{photon} = 304 \pm 41$ MeV

$\varepsilon(1\ \text{fm}/c) \approx 14$ GeV/fm^3

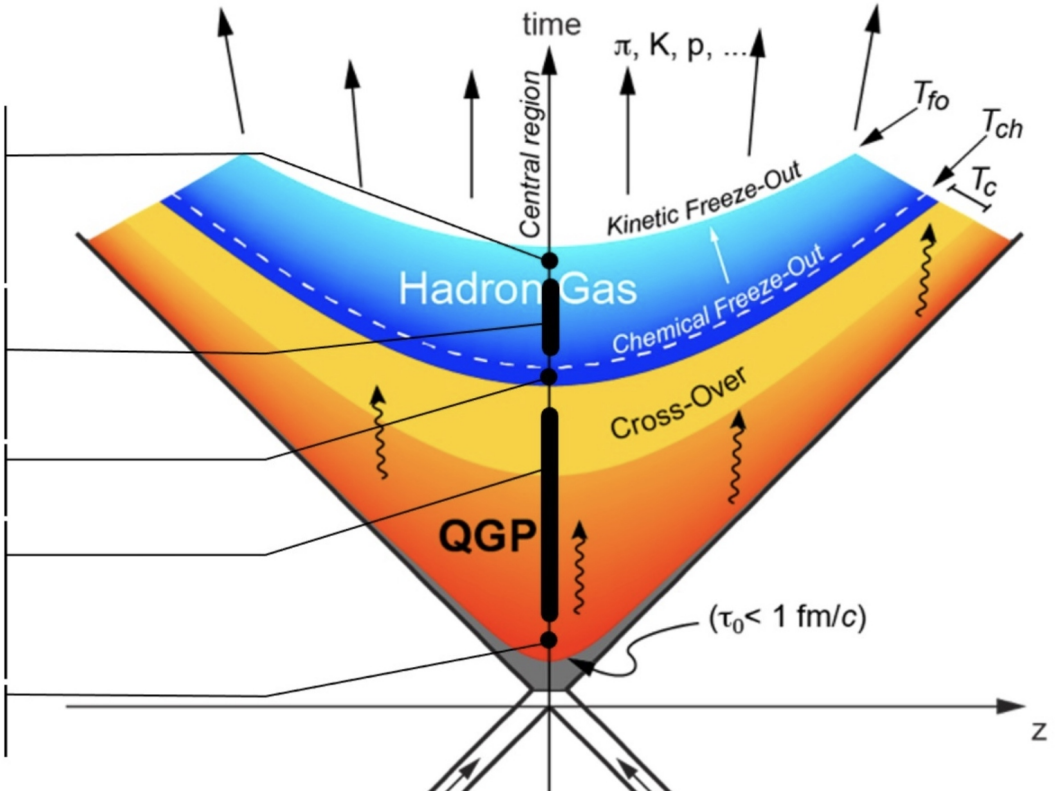

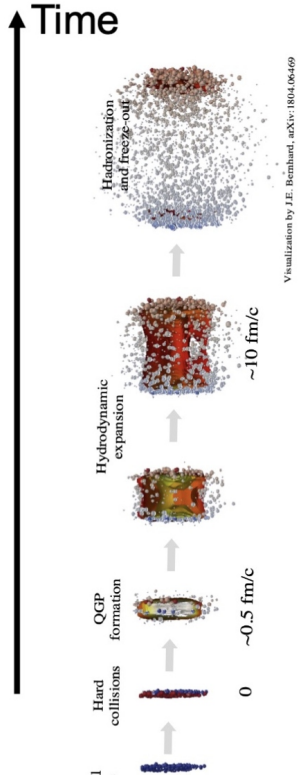

some open issues

- SHM and QCD
- SHM and loosely bound states
- SHM and small collision system
- SHM and hyper-triton

SHM and QCD

1. SHM is defined for temperatures equal or less than the temperature of the QCD phase transition

2. the equation of state of SHM is that of the hadron resonance gas HRG, significant systematic uncertainties result from incomplete knowledge of the full HRG spectrum, especially in the charm and beauty sector

3. hadron formation is implemented as sudden ‘Cooper-Frye’ freeze-out

4. SHM is not applicable for particle production in the universe

5. after freeze-out, the HRG is out of equilibrium

SHM and loosely bound objects: the hyper-triton
discovered in 1952/1953

mass = 2990 MeV, binding energy = 2.3 MeV

Lambda sep. energy = 0.10 MeV

molecular structure: (p+n) + Lambda

2-body threshold: (p+p+n) + pi- = ^{3}He + pi-

rms radius = (4 B.E. M_{red})$^{-1/2}$ = 10.3 fm =
rms separation between d and Lambda

in that sense: hypertriton = (p n Lambda) =
(d Lambda) is the ultimate halo state

bound state >> system size unsolved open issue

see also recent ALICE paper 2604.07949 [nucl-ex]

hypernuclei – discovery and 1st measurements of hypertriton

M. Danysz, J. Pniewski, Philos. Mag. 44 (1953) 348.
D.A. Tidman, et al., Philos. Mag. 44 (1953) 350.
J. Crussard, D. Morellet, C. R. Acad. Sci. Paris 236 (1953) 64.
A. Bonetti, et al., Nuovo Cimento 11 (1954) 210;
A. Bonetti, et al., Nuovo Cimento 11 (1954) 330.

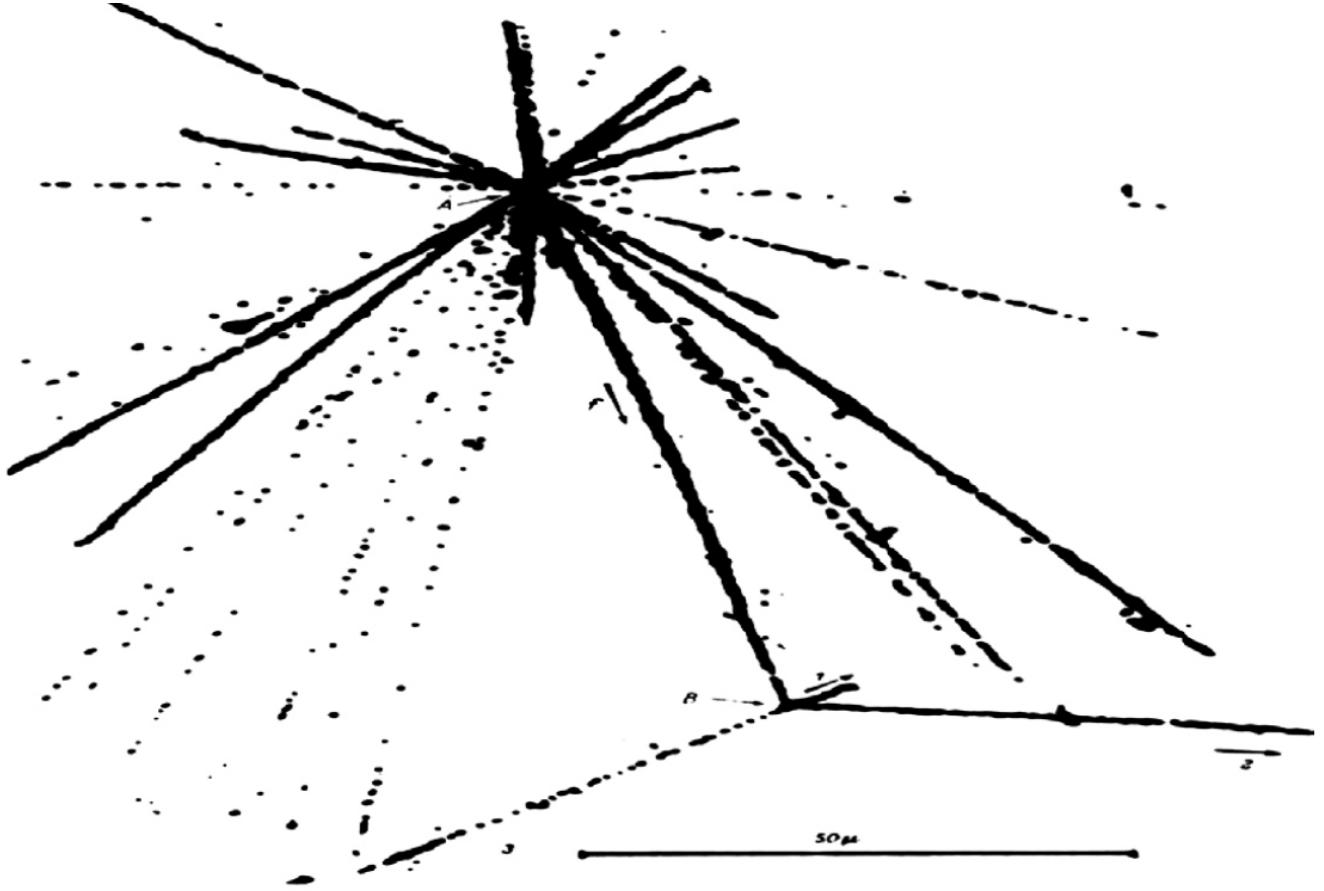

B meson tracking down to very low transverse momentum

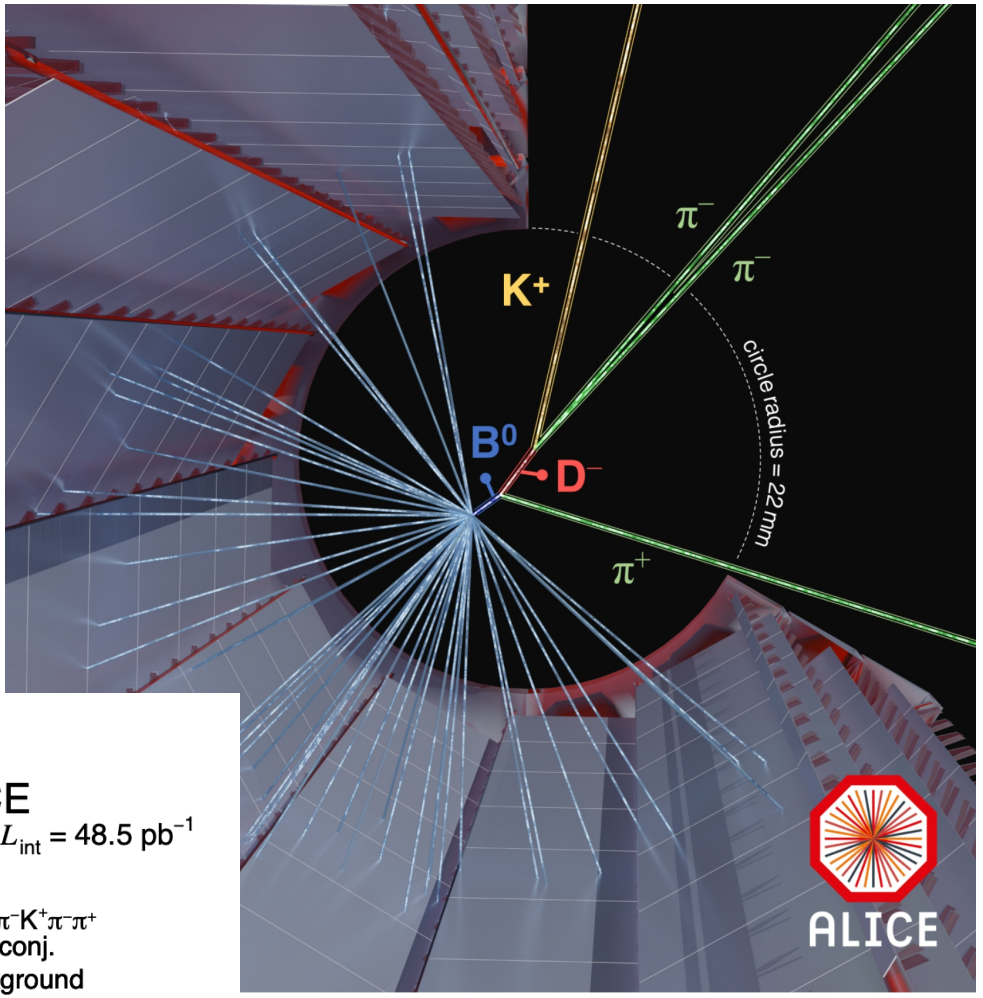

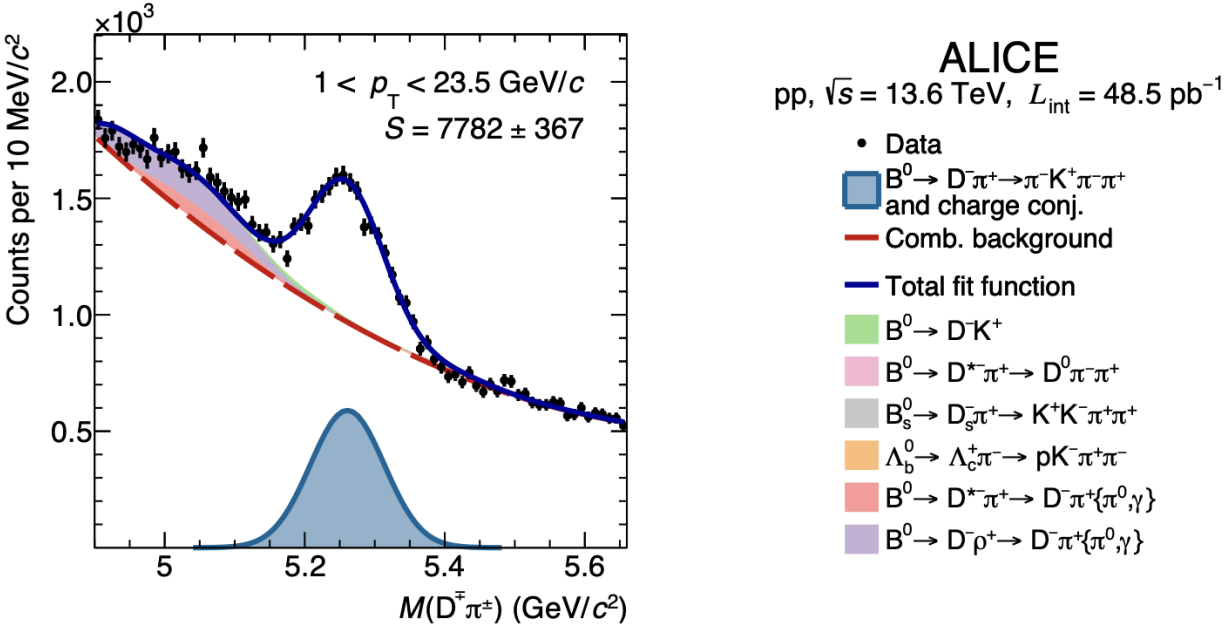

SHM and hypertriton

hypertriton, the most exotic bound state in the nuclear data table, a very fragile bound state made of a deuteron and a Lambda-hyperon with huge size

to form such objects via the short range (1-2 fm) interaction the process must start in an early, compact configuration, independent of whether coalescence or SHM is at work

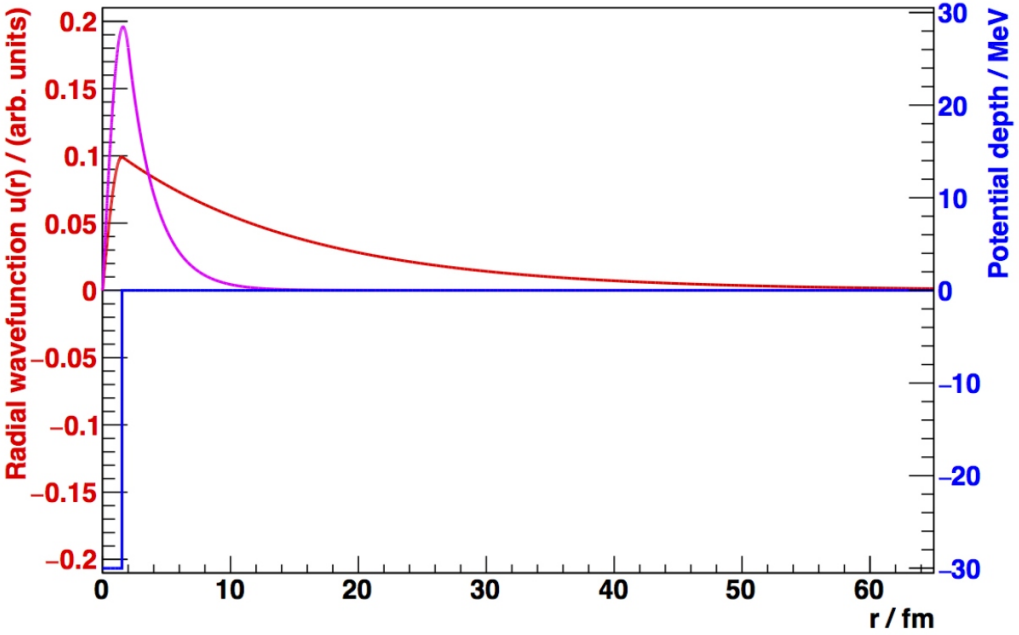

Wave function (red) of the hypertriton assuming a s-wave interaction for the bound state of a Λ and a deuteron. The root mean square value of the radius of this function is $\sqrt{\langle r^2 \rangle} = 10.6$ fm. In blue the corresponding square well potential is shown. In addition, the magenta curve shows a "triton" like object using a similar calculation as for the hypertriton, namely a deuteron and an added nucleon, resulting in a much narrower object.

pbm and B. Doenigus

Nucl.Phys.A 987 (2019) 144-201, 1809.04681 [nucl-ex]

very different wave functions for bound states with baryon number 2 and 3

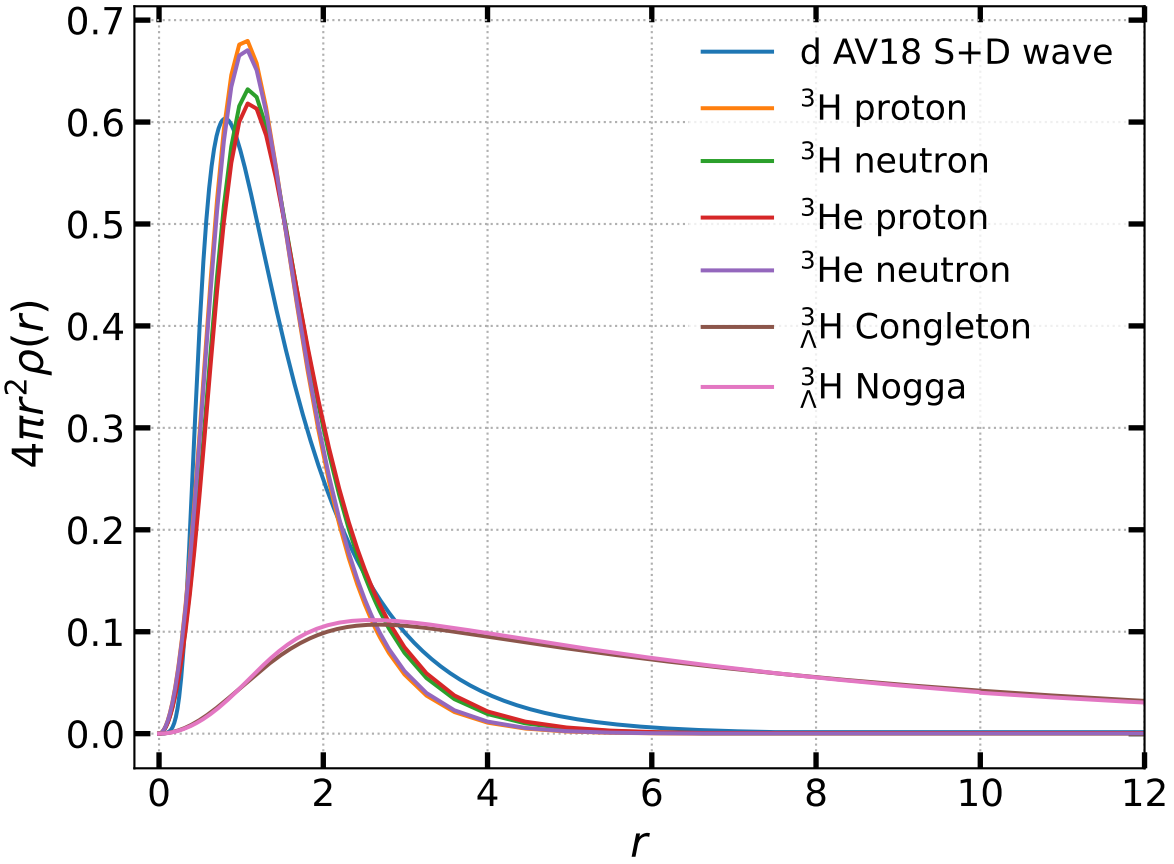

results of very recent microscopic calculations

for references, see A. Andronic, pbm, H. Brunssen, J. Stachel, to appear

hypertriton properties

ALICE coll.,

Phys. Rev. Lett. 131 (2023) 10, 102302

The most precise measurements to date of the ${}^{3}_{\Lambda}\mathrm{H}$ lifetime τ and Λ separation energy B_{Λ} are obtained using the data sample of Pb–Pb collisions at $\sqrt{s_{\mathrm{NN}}} = 5.02$ TeV collected by ALICE at the LHC. The ${}^{3}_{\Lambda}\mathrm{H}$ is reconstructed via its charged two-body mesonic decay channel (${}^{3}_{\Lambda}\mathrm{H} \rightarrow {}^{3}\mathrm{He} + \pi^{-}$ and the charge-conjugate process). The measured values $\tau = [253 \pm 11\ (\mathrm{stat.}) \pm 6\ (\mathrm{syst.})]$ ps and $\mathrm{B}_{\Lambda} = [102 \pm 63\ (\mathrm{stat.}) \pm 67\ (\mathrm{syst.})]$ keV are compatible with predictions from effective field theories and confirm that the ${}^{3}_{\Lambda}\mathrm{H}$ structure is consistent with a weakly-bound system.

hypertriton and anti^{3}He measurements with ALICE @ LHC

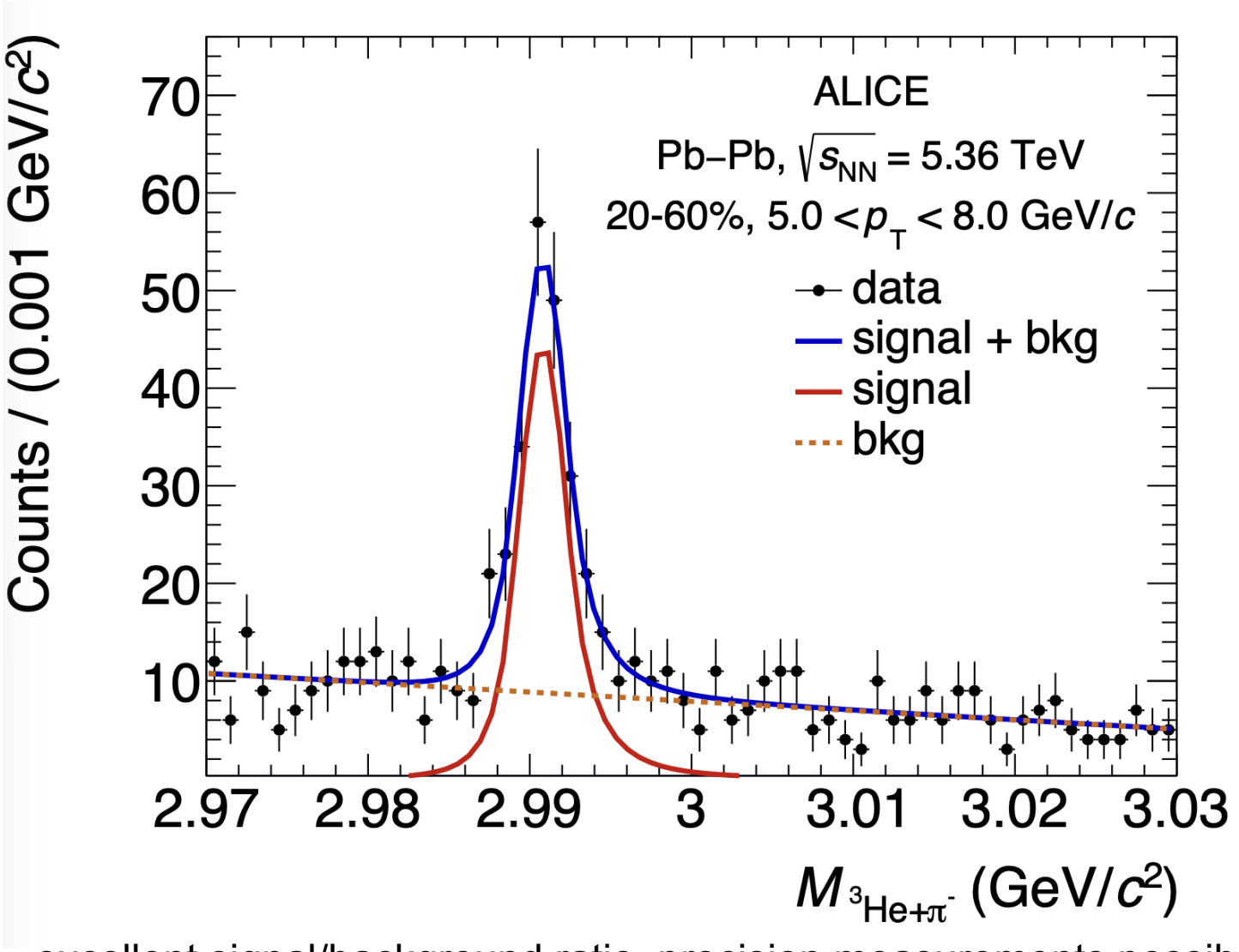

excellent signal/background ratio, precision measurements possible
2026 data have even better mass resolution

azimuthal anisotropy measurements for determination of hydrodynamic flow

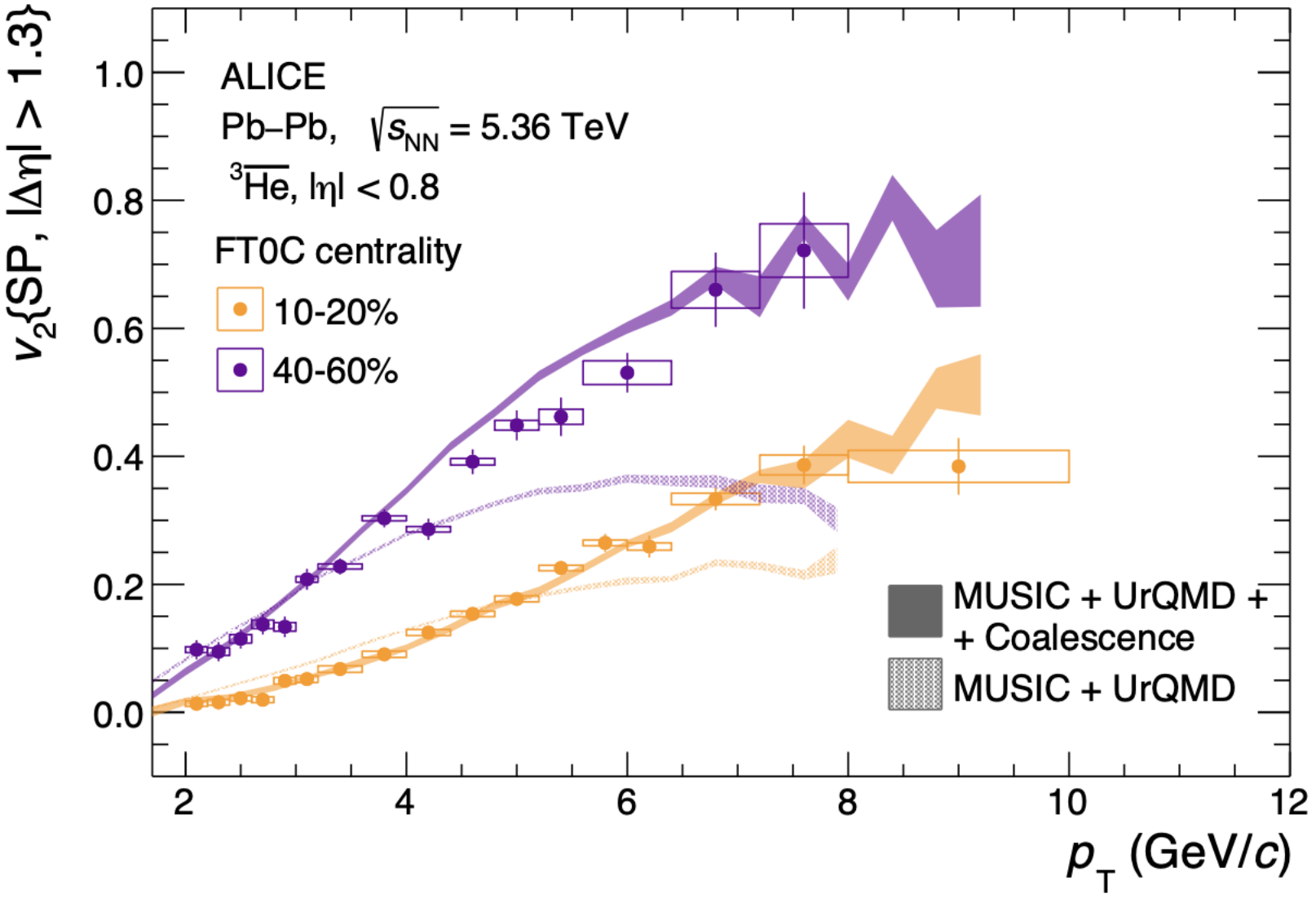

towards precision flow measurements

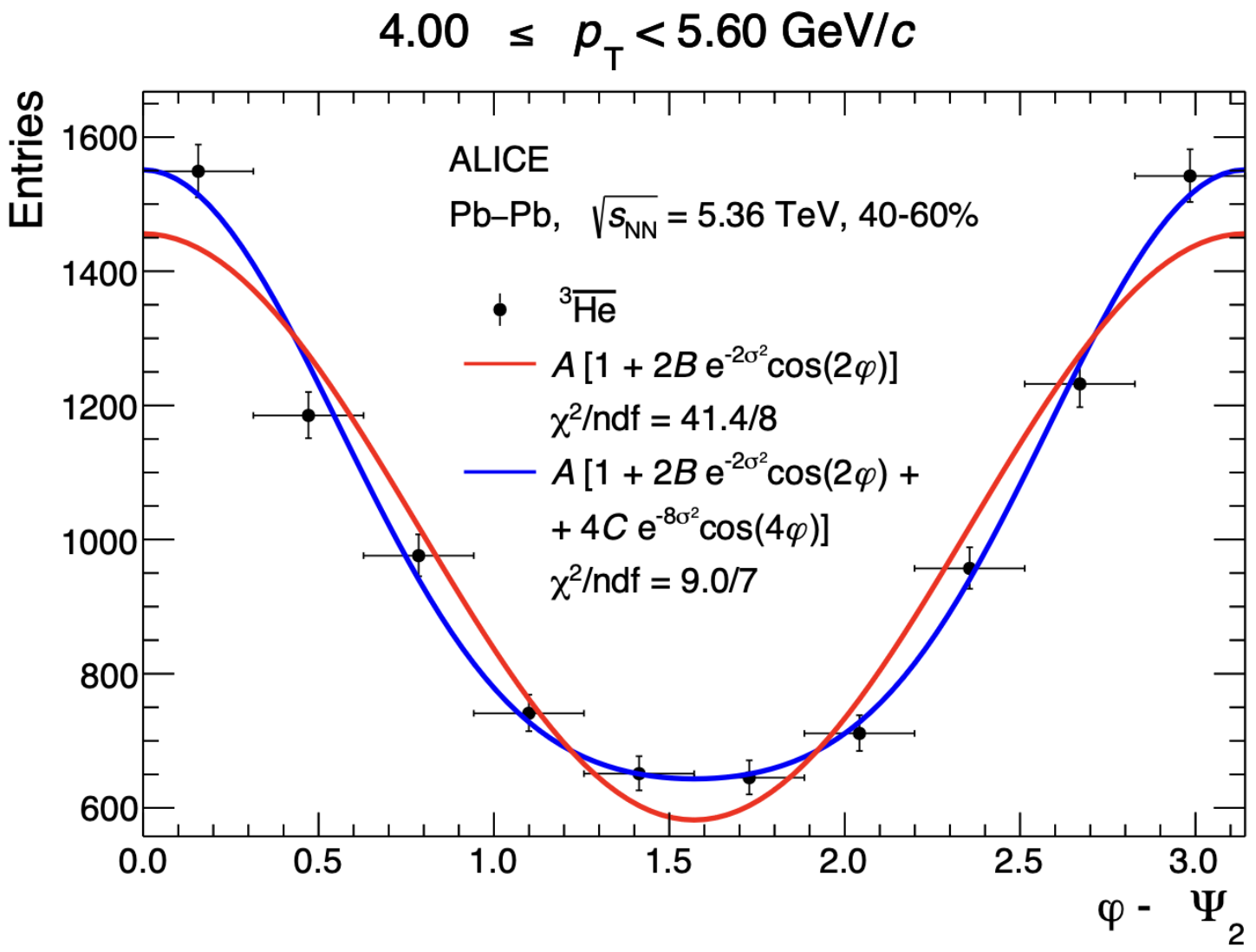

even 4th moment measured with precision

comparison anti^{3}He and hypertriton flow

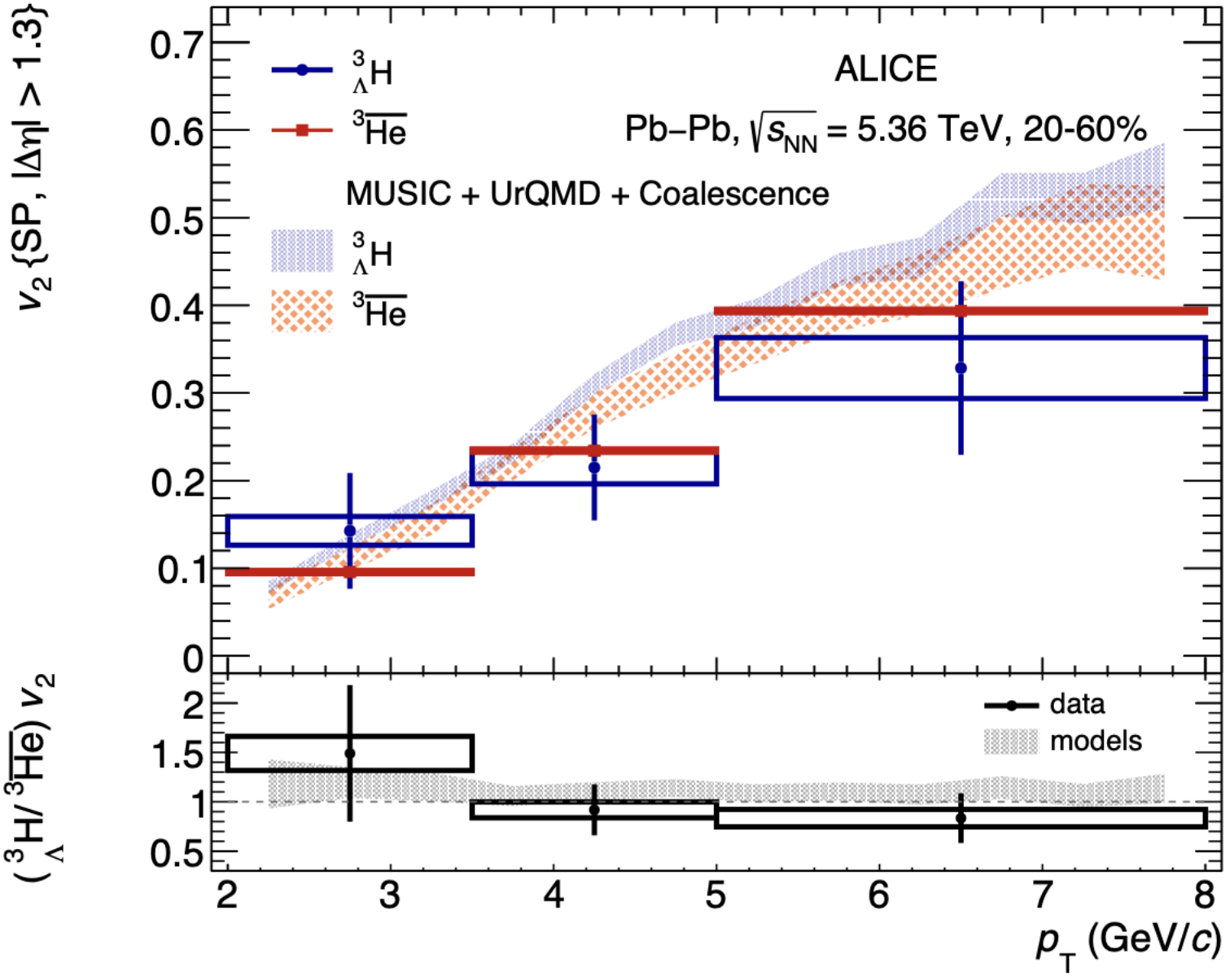

2603.19398 [nucl-ex]

summary of flow measurements with anti^{3}He and hypertriton

- anti^{3}He and hypertriton in Pb—Pb collisions have nearly the same mass and exhibit very similar flow
- anti^{3}He and hypertriton have dramatically different wave functions
- apparently no wave function sensitivity in Pb—Pb as expected in thermal (SHM) description
- how to understand apparent strong wave function sensitivity for hypertriton production in pp collisions? see recent ALICE paper 2604.07949 [nucl-ex]?

schematic size correction

inspired by Berndt Mueller, SQM2022, arXiv:2209.00070A.

see A. Andronic, pbm, H. Brunssen, J. Stachel, to appear

$$\mathcal{S}_i = \frac{1}{V_{\Delta y=1}} \int_{V_{\Delta y=1}} \mathrm{d}^3 x_1 \int_{V_{\Delta y=1}} \mathrm{d}^3 x_2 \left|\psi_i(\mathbf{x}_1 - \mathbf{x}_2)\right|^2$$

$V_{\Delta y=1}$ is the volume of the fireball for 1 unit of rapidity and for a 2-body bound state like the deuteron, the wave function is the p-n relative wavefunction.

if |**x1** – **x2**| << size of the fireball, the correction is unity

size dependence for Λ baryon as test

all data from ALICE, refs. available on request

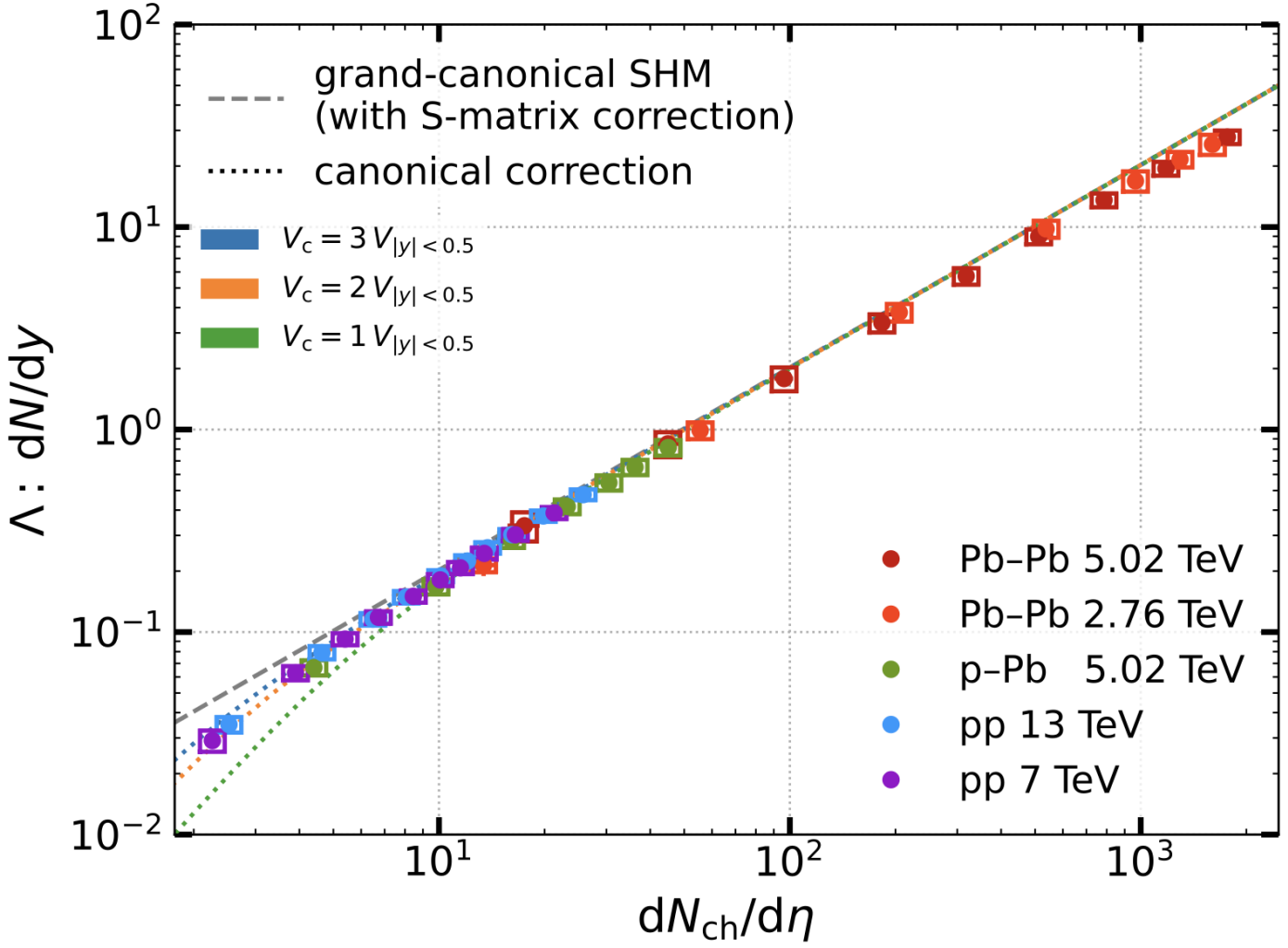

A. Andronic, pbm, H. Brunssen, J. Stachel, to appear

Multiplicity dependence of Λ yields. Grand-canonical SHM, canonical suppression and additionally size-corrected predictions are drawn as grey dashed, dotted and solid lines, respectively, with colors indicating different values of V_c.
Error bars (open boxes) represent statistical (systematic) uncertainties.

SHM and loosely bound states

1. SHM works well for composite objects such as deuterons or light nuclei

2. deuteron is a loosely bound state (B.E. = 2.2 MeV << reduced mass)

3. very few parameters, canonical correction needs (strangeness or charm) correlation length

4. at LHC energy, SHM works well for small and large collision systems

5. canonical thermodynamics is applied and crucial for low multiplicities

6. applying size correction as proposed by Berndt Mueller,SQM2022, arXiv:2209.00070 does not describe system size dependence

7. for a 2-body s-wave bound state with vanishing binding energy, the wave function becomes universal, independent of nuclear potentials etc. see, e.g. Artoisenet & Braaten, Phys. Rev. D83 (2011) 014015.

this implies
rms radius = $(4\ \text{B.E.}\ M_{red})^{-1/2}$
= 3 fm for deuteron
formation time proportional to 1/B.E.
about 100 fm for deuteron
>> 100 fm for '2-body'
hyper-triton

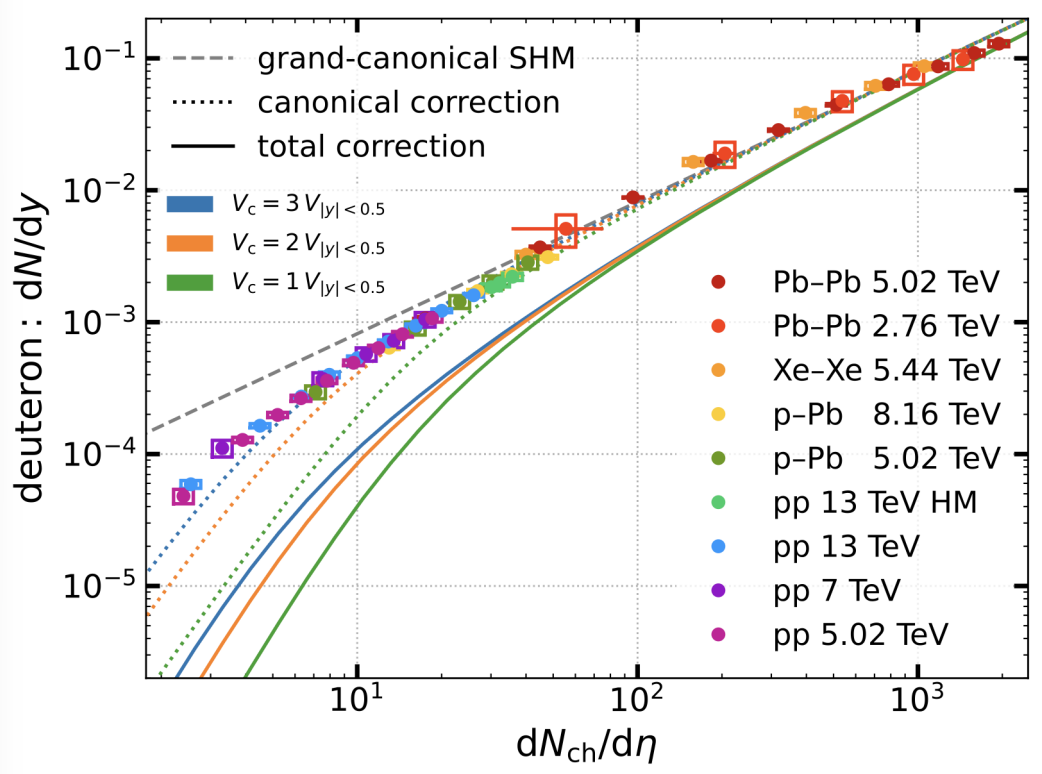

A. Andronic, pbm, H. Brunssen, J. Stachel, to appear

^{3}He calculations as function of associated charge multiplicities

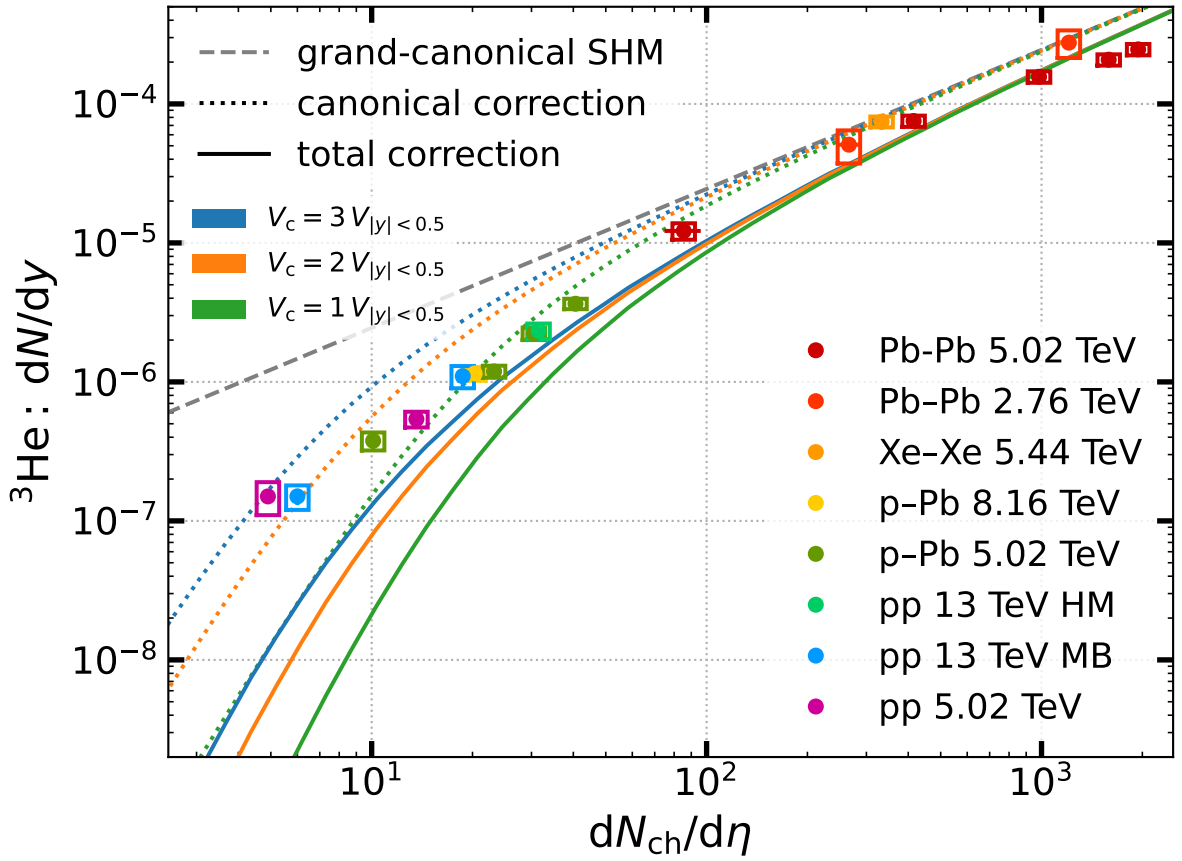

A. Andronic, pbm, H. Brunssen, J. Stachel, to appear

the complicated case of hypertriton

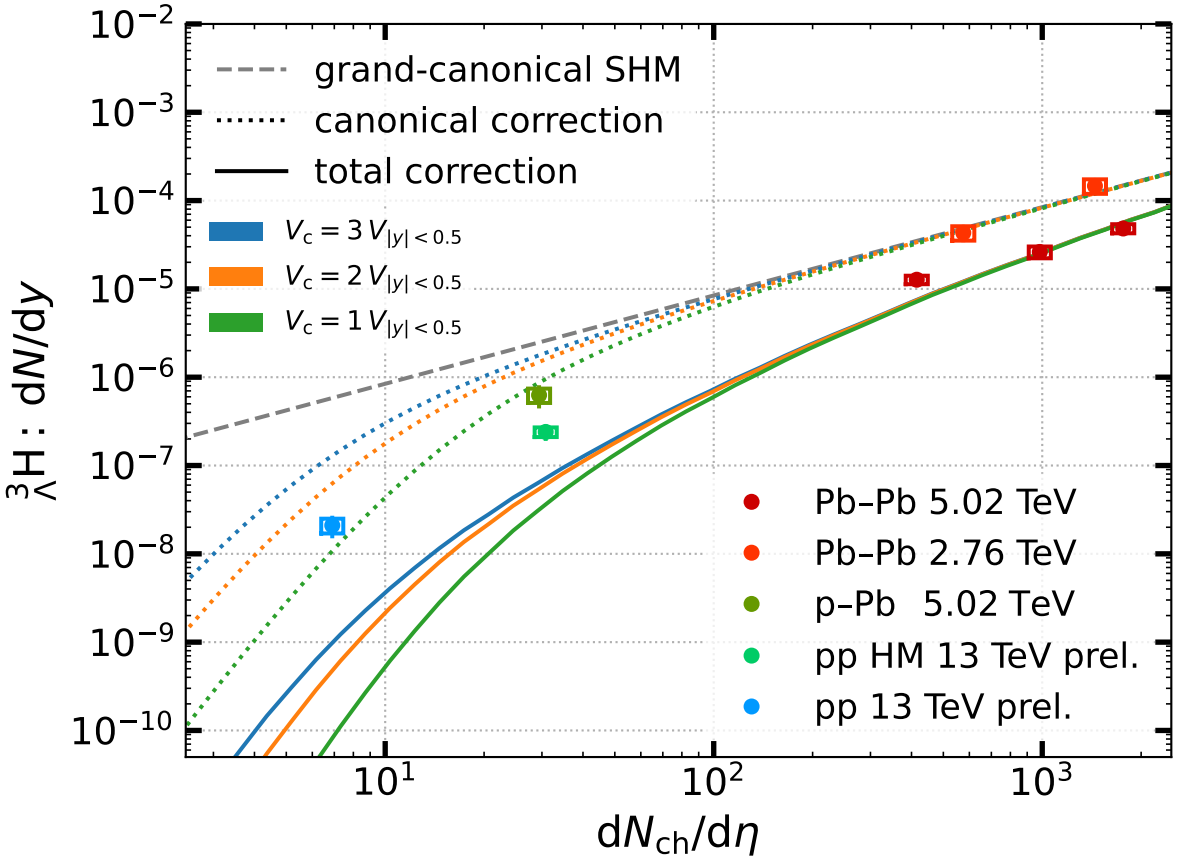

A. Andronic, pbm, H. Brunssen, J. Stachel, to appear

summary: SHM

very useful for description of hadron yields and higher moments

extended to charm and beauty sector (balance equation)

contains HRG equation of state

coupled to hydro models for p_T spectra

with canonical correction, good description also for deuteron and A = 3 nuclei in all collision systems

open issue: hyper-triton production, yields, flow, dependence on system size

high precision and statistics data from LHC Run4 and from new experiment ALICE 3 in LHC Run5 will hopefully shed light on this

happy birthday, and many, many returns!!!

backup

Observation of Anisotropic Event Shapes and Transverse Flow in Au+Au Collisions at AGS Energy

J. Barrette[4], R. Bellwied[8], S. Bennett[8],
P. Braun-Munzinger[6], W. E. Cleland[5], M. Clemen[5],
J. Cole[3], T. M. Cormier[8], G. David[1], J. Dee[6],
O. Dietzsch[7], M. Drigert[3], S. Gilbert[4], J. R. Hall[8],
T. K. Hemmick[6], N. Herrmann[2], B. Hong[6], C. L. Jiang[6],
Y. Kwon[6], R. Lacasse[4], A. Lukaszew[8], Q. Li[8],
T. W. Ludlam[1], S. McCorkle[1], S. K. Mark[4], R. Matheus[8],
E. O'Brien[1], S. Panitkin[6], T. Piazza[6], C. Pruneau[8],
M. N. Rao[6], M. Rosati[4], N. C. daSilva[7], S. Sedykh[6],
U. Sonnadara[5], J. Stachel[6], H. Takai[1], E. M. Takagui[7],
S. Voloshin[5], G. Wang[4], J. P. Wessels[6], C. L. Woody[1],
N. Xu[6], Y. Zhang[6], Z. Zhang[5], C. Zou[6]

(E877 Collaboration)

[1] *Brookhaven National Laboratory, Upton, NY 11973*
[2] *Gesellschaft für Schwerionenforschung, Darmstadt, Germany*
[3] *Idaho National Engineering Laboratory, Idaho Falls, ID 83402*
[4] *McGill University, Montreal, Canada*
[5] *University of Pittsburgh, Pittsburgh, PA 15260*
[6] *SUNY, Stony Brook, NY 11794*
[7] *University of São Paulo, Brazil*
[8] *Wayne State University, Detroit, MI 48202*

Event shapes for Au + Au collisions at 11.4 GeV/c per nucleon were studied over nearly the full solid angle with the E877 apparatus. The analysis was performed by Fourier expansion of azimuthal distributions of the transverse energy (E_T) measured

experimental discovery of elliptic flow and higher Fourier moments at AGS
Phys.Rev.Lett. 73 (1994) 2532-2535

7 years before RHIC

$$x_n = \int_0^{2\pi} r(\phi)\cos(n\phi)d\phi = \sum_\nu r_\nu \cos(n\phi_\nu),$$

$$y_n = \int_0^{2\pi} r(\phi)\sin(n\phi)d\phi = \sum_\nu r_\nu \sin(n\phi_\nu),$$

$$v_n = \sqrt{x_n^2 + y_n^2}$$

theory paper:
S. Voloshin, Y. Zhang,
Z.Phys. C 70 (1996) 665-672, 1144 citations

fast forward to the collider regime

- 2000 start of RHIC operation
- Gyulassy & McLerran review Nucl. Phys. A 750 (2005) 30-63
- 2009 start of LHC operation
- ALICE review Eur. Phys. J. C 84 (2024) 8, 813

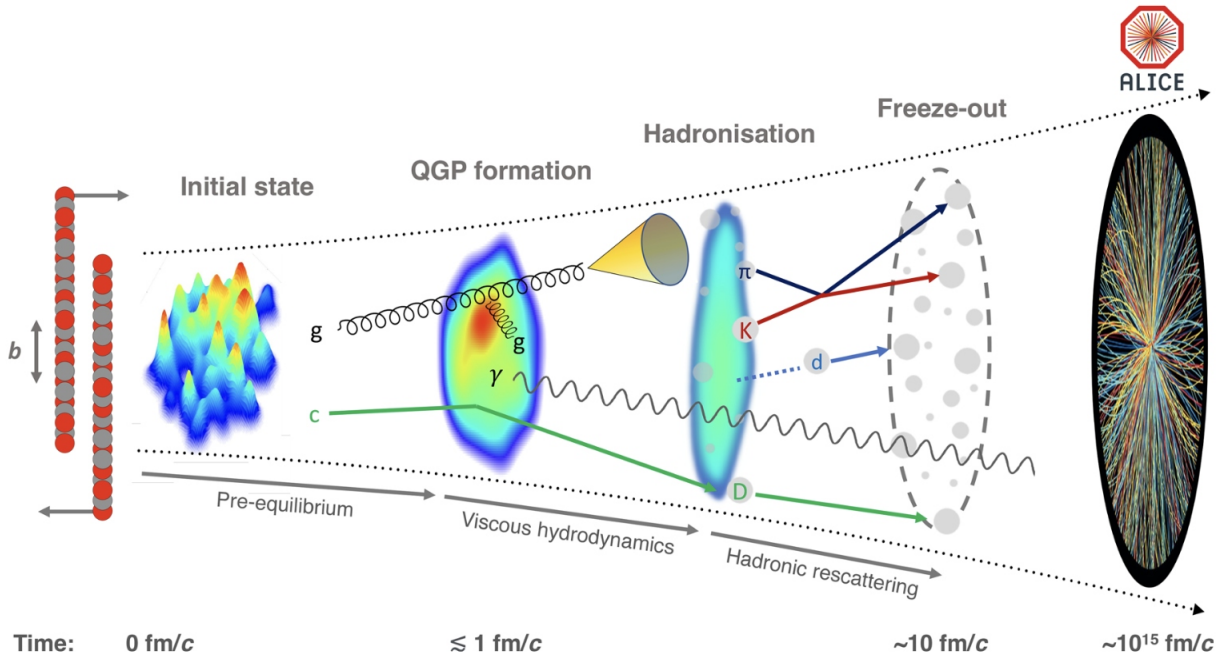

The evolution of a heavy-ion collision at LHC energies

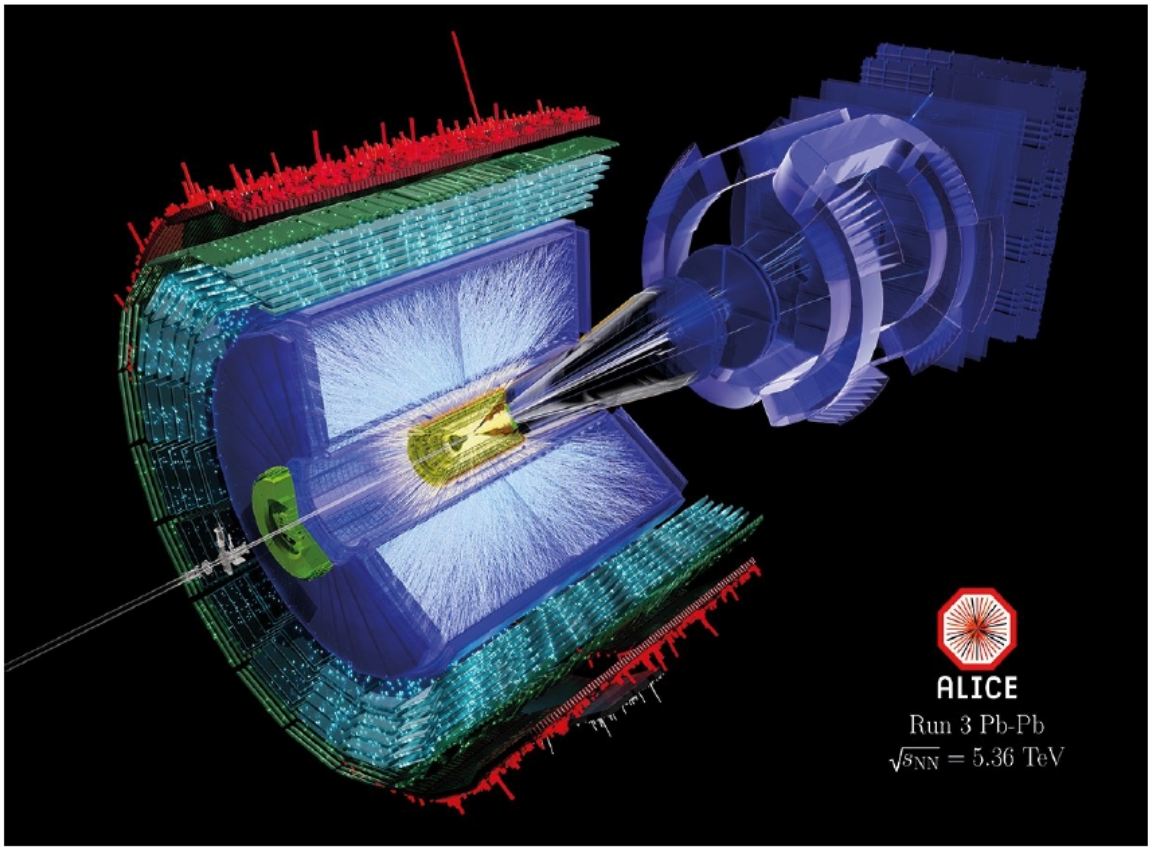

ALICE in 2023 Run 3

QCD phase diagram from 'statistical hadronization model'

update 2025

hadronic matter cannot be heated to T > T_{CF} even at LHC energy

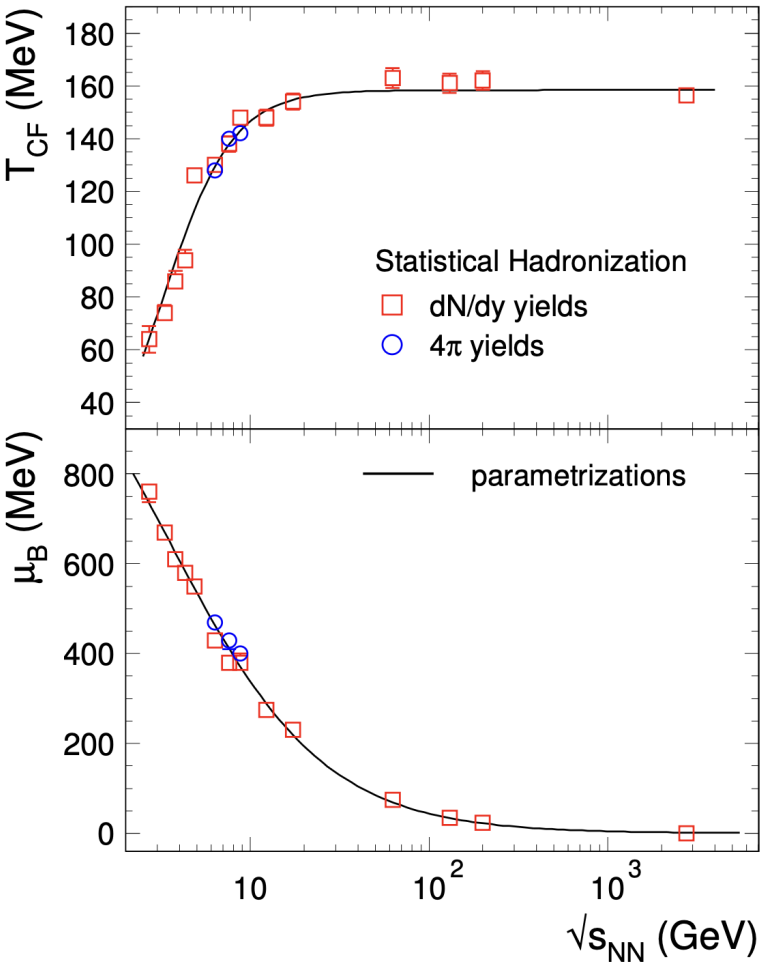

Tpc = 156 MeV

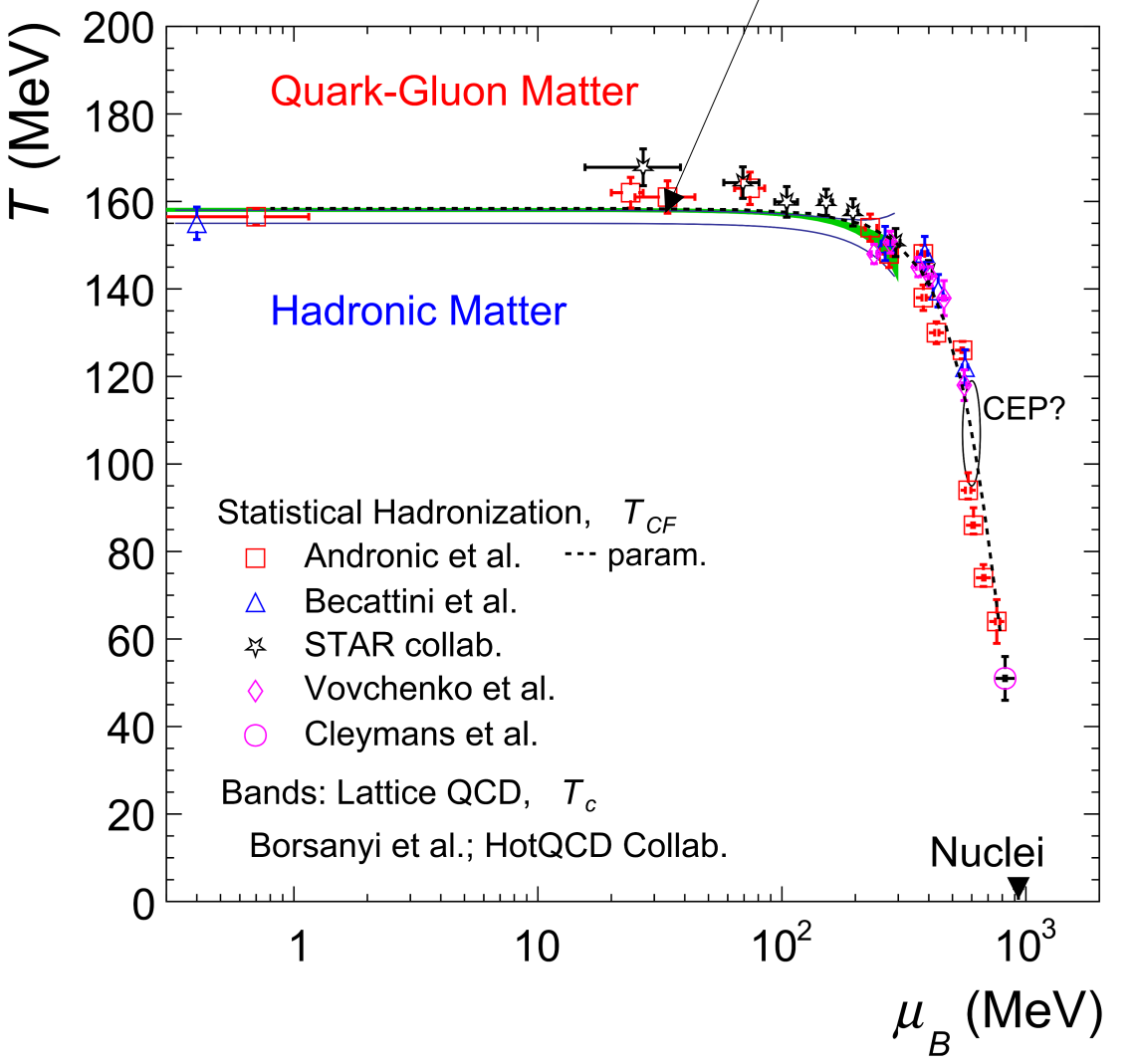

lattice predictions in quantitative agreement with results from statistical hadronization model,

CEP from Phys. Rev.D 111 (2025) 3, L031502

Canonical thermodynamics and fluctuations of proton distributions in ultra-relativistic nuclear collisions

recent data from STAR and HADES compared to predictions based on uncorrelated production and baryon number conservation

deviations from this ‘canonical baseline’ could be indications for new dynamical effects (onset of 1st order phase transition?)

Factorial cumulant ratios, $C_2(p)/C_1(p)$

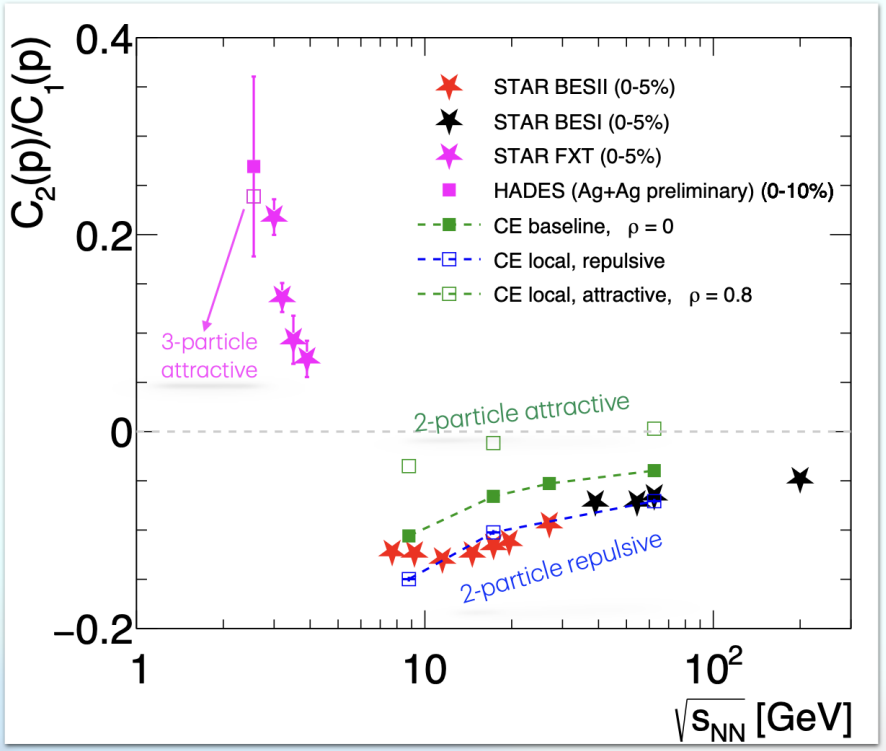

- Strong **non-monotonic** energy dependence
- **Change of sign** towards lower energies
- Consistent results between **STAR** and **HADES**

STAR FXT: Au-Au, $\langle N_W \rangle \approx 320$:
$-0.5 < y < 0$
$0.4 < p_t < 2$ GeV/c

HADES: Ag-Ag, $\langle N_W \rangle \approx 170$
$-0.4 < y < 0.4$
$0.4 < p_t < 1.6$ GeV/c

The interplay of repulsive and attractive forces between protons explains the measured energy dependence

STAR: Zachary Sweger, Shinichi Esumi, Quark Matter 25
HADES: Marvin Nabroth, Quark Matter 25

P. Braun-Munzinger, B. Friman, K. Redlich, A. Rustamov, J. Stachel, NPA 1008 (2021) 122141
P. Braun-Munzinger, K. Redlich, A. Rustamov, J. Stachel, JHEP 08 (2024) 113
B. Friman, A. Rustamov, K. Redlich (in preparation)

Slide prepared by Anar Rustamov

new ALICE development: strangeness tracking for multi-charm baryons

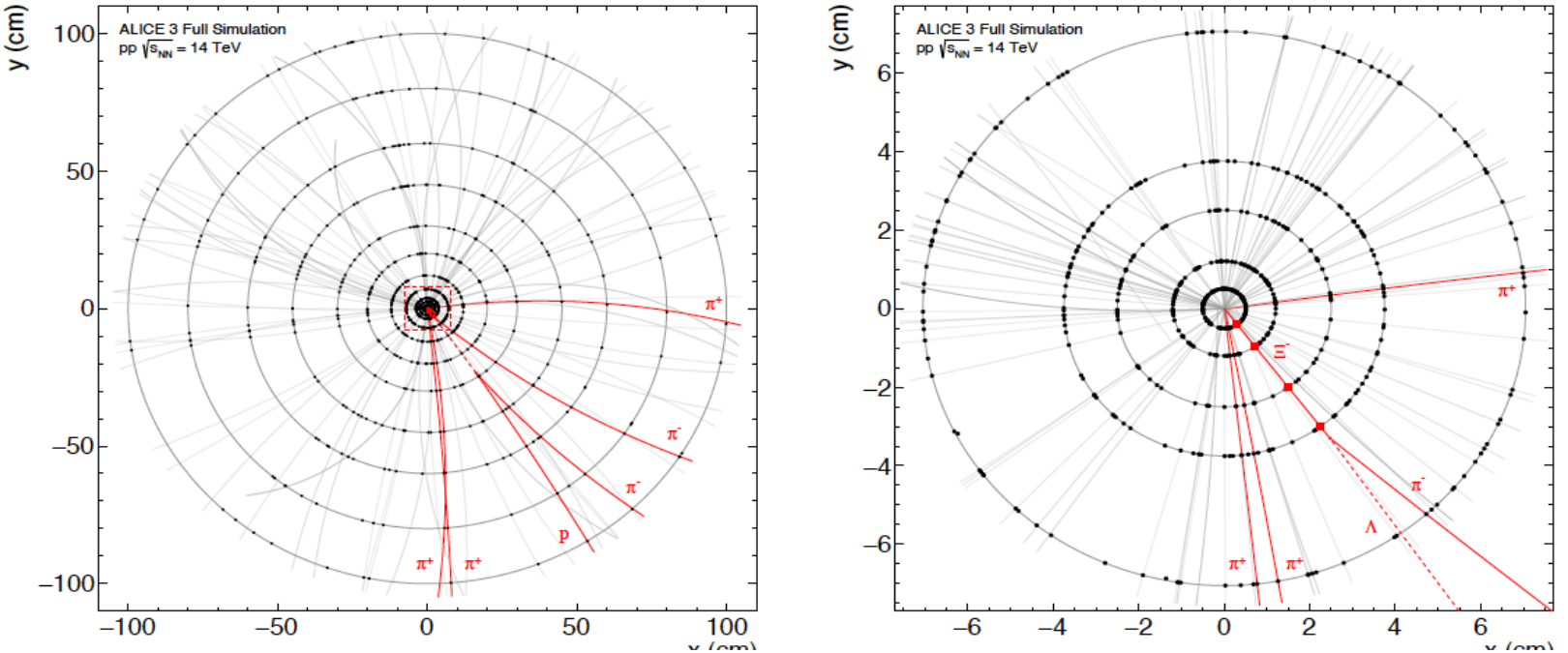

(left) Illustration of strangeness tracking from full detector simulation of the Ξ_{cc}^{++} decay into $\Xi_c^+ + \pi^+$ with the successive decay $\Xi_c^+ \to \Xi^- + 2\pi^+$. (right) Close-up illustration of the region marked with a red dashed box in the left figure, containing the five innermost layers of ALICE 3 and the hits that were added to the Ξ^- trajectory (red squares).

Ξ^{++}_{cc} mass spectrum without (red) and with (blue) strangeness tracking

the power of ultra-thin, ultra-precise MAPS detectors for ALICE 3

first successful tests with data in Run3 are now available

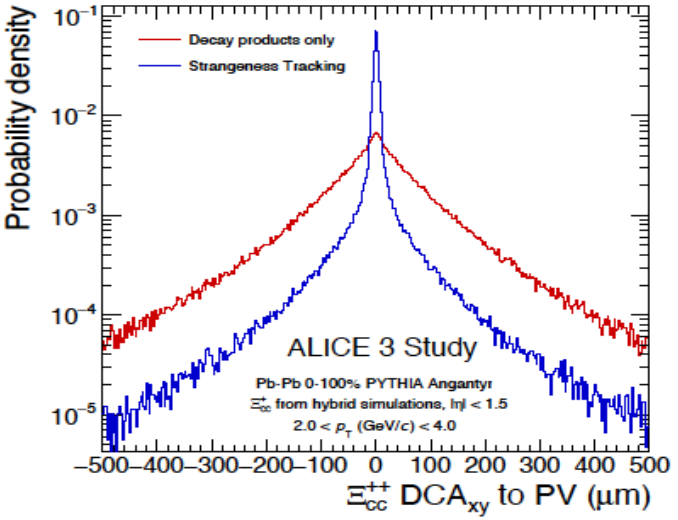

ALICE plans and status for the coming decade 2025 – 2034
LHC Run3 and Run4

ALICE upgrade 2019 - 2021:

GEM based read-out chambers for the TPC, new inner tracker with ultra-thin Si layers, continuous read of (all) subdetectors

increase of data rates by factor >50

focus on rare objects, exotic quarkonia, single (and possibly double) charm hadrons to address a number of fundamental questions and issues such as:

- what is the deconfinement radius for charm quarks
- are there colorless bound states in a deconfined medium?
- are complex, light nuclei and exotic charmonia (X,Y,Z) produced as compact multi-quark bags?
- can fluctuation measurements shed light on the mechanism of baryon production and critical behavior near the phase boundary?

- low mass dileptons and low-p_T thermal photons
- collectivity from pp to AA collisions
- nuclear and hadronic physics
  - structure of light hyper-nuclei
  - hadron-hadron interaction from particle correlations
- ultra-peripheral and diffractive collisions

deciphering QCD in the strongly coupled regime

ALICE in Run 3 (ongoing)

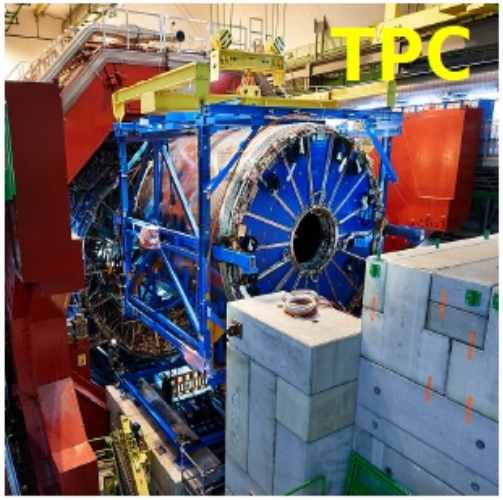

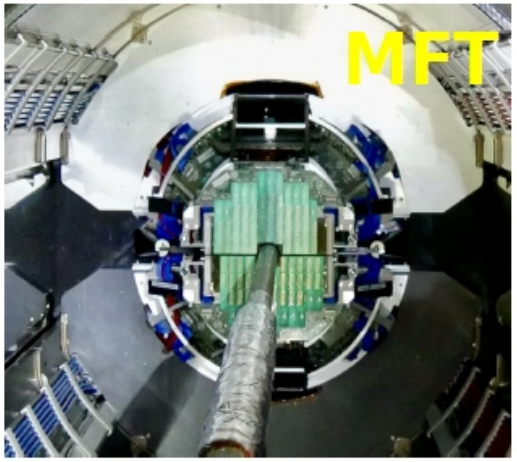

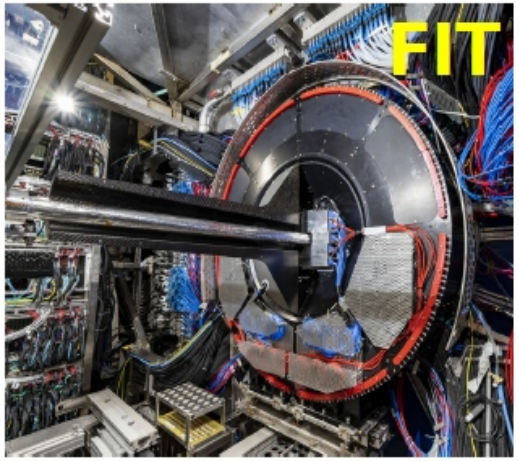

- Major upgrades installed in 2019-2021
- In production since 2022
- 50x increase in readout rate
- 3 to 6x improvement in pointing resolution
- Secondary vertexing for forward muons

ALICE upgrades: *arXiv:2302.01238*
ITS: *NIM 1032(2022)166632*
TPC: *JINST 16 P03022 (2021)*
MFT: *CDS link*
FIT: *NIM 1039 (2022) 167021*

the mechanism for statistical hadronization with charm (SHMc)

[Braun-Munzinger and Stachel, PLB 490 (2000) 196]
[Andronic, Braun-Munzinger and Stachel, NPA 789 (2007) 334]

- Charm quarks are produced in initial hard scatterings ($m_{c\bar{c}} \gg T_c$) and production can be described by pQCD ($m_{c\bar{c}} \gg \Lambda_{QCD}$)
- Charm quarks survive and *thermalise* in the QGP
- Full screening before T_{CF}
- Charmonium is formed at phase boundary (together with other hadrons)
- Thermal model input ($T_{CF}, \mu_b \rightarrow n_X^{th}$)

$$N_{c\bar{c}}^{dir} = \underbrace{\frac{1}{2} g_c V \left(\sum_i n_{D_i}^{th} + n_{\Lambda_i}^{th} + \cdots \right)}_{\text{Open charm}} + \underbrace{g_c^2 V \left(\sum_i n_{\psi_i}^{th} + n_{\chi_i}^{th} + \cdots \right)}_{\text{Charmonia}}$$

- Canonical correction is applied to n_{oc}^{th}
- Outcome $N_{J/\psi}, N_D, \ldots$

core-corona picture: treat low density part of nuclear overlap region, where a nucleon undergoes 1 or less collisions as pp collisions, use measured pp cross section scaled by $T_{AA} = N_{coll}/\sigma_{inel}^{pp}$ with N_{coll} the number of (hard) collisions as obtained in the Glauber approach

J/ψ and statistical hadronization

arXiv: 2303.13361

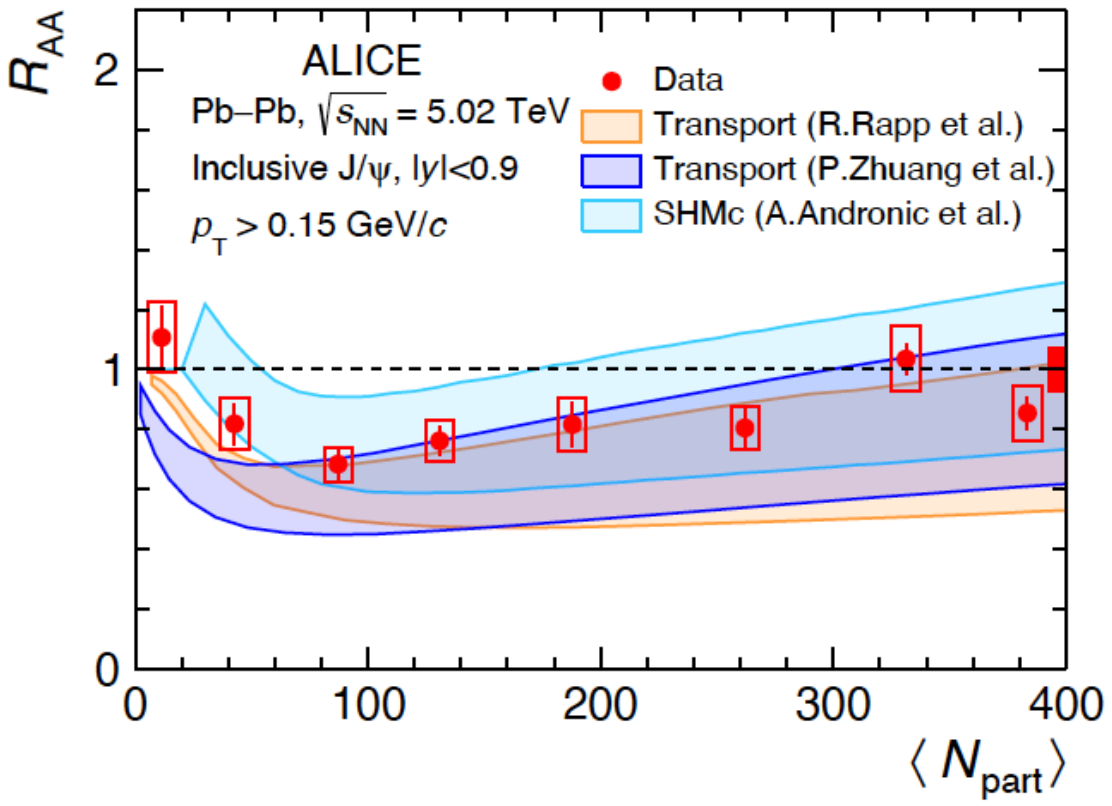

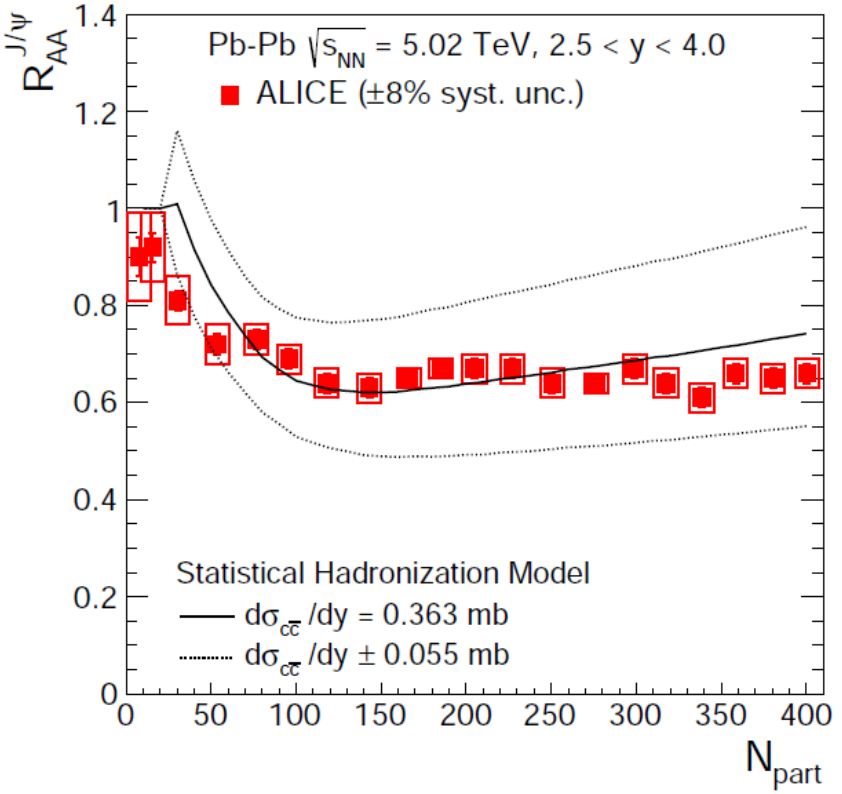

production in PbPb collisions at LHC consistent with deconfinement and subsequent statistical hadronization within present uncertainties
main uncertainty: open charm cross section

beyond yields: transverse momentum distributions coupling SHMc with relativistic hydrodynamics

arXiv:2308.16125

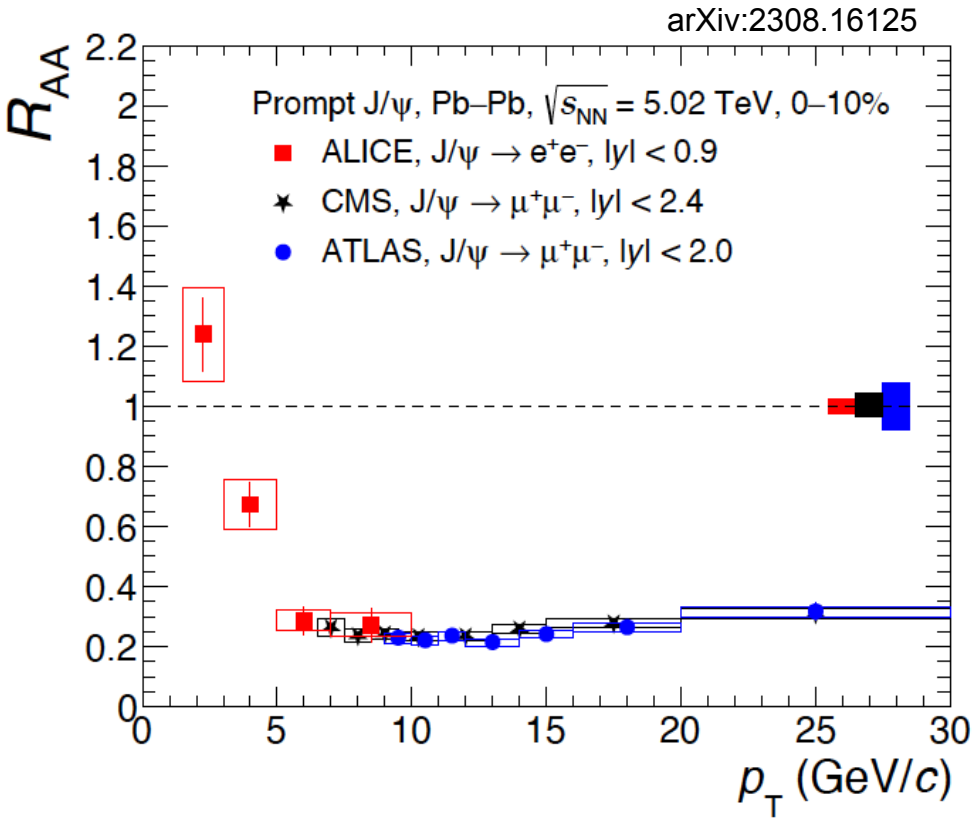

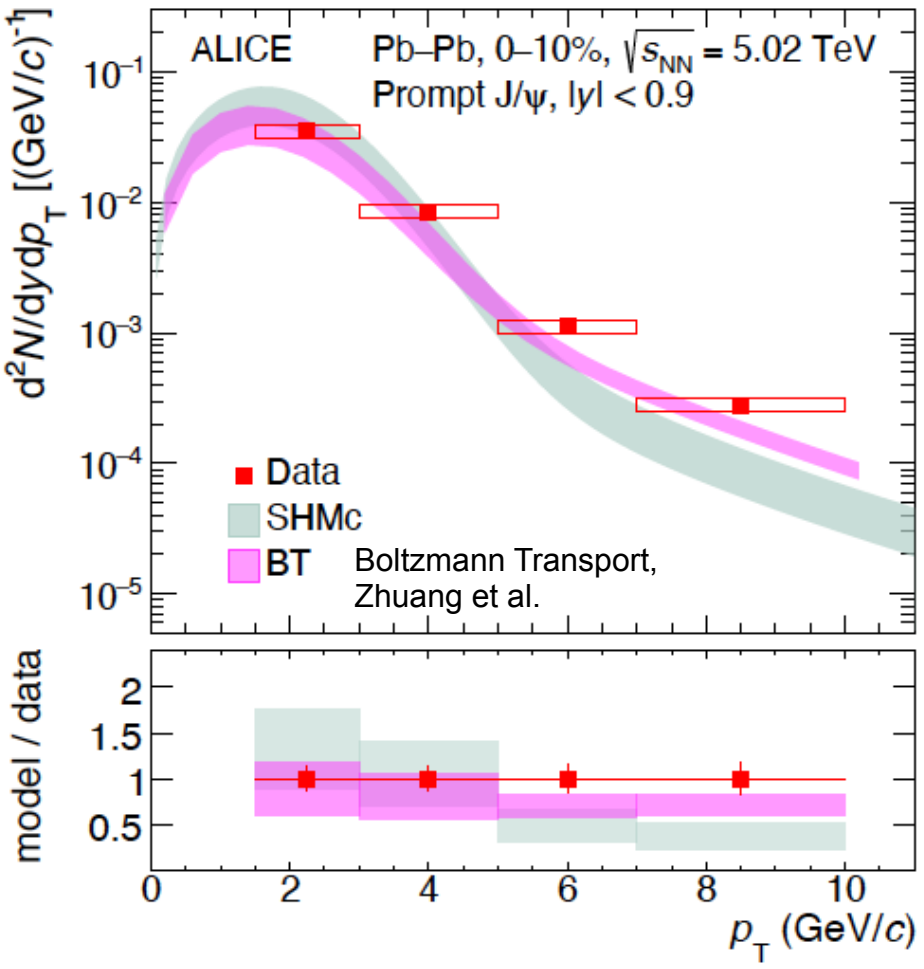

new ALICE: separation of prompt and nonprompt J/ψ down to 1.3 GeV/c

enhancement strongly rising towards lower p_t even beyond pp
(not even considering shadowing)

New approach to spectra: implement charmonia into hydrodynamics codes directly

A. Andronic, P. Braun-Munzinger, J. Brunßen, J. Crkovska, J. Stachel, V. Vislavicius, M. Völkl, arXiv: 2308.14821

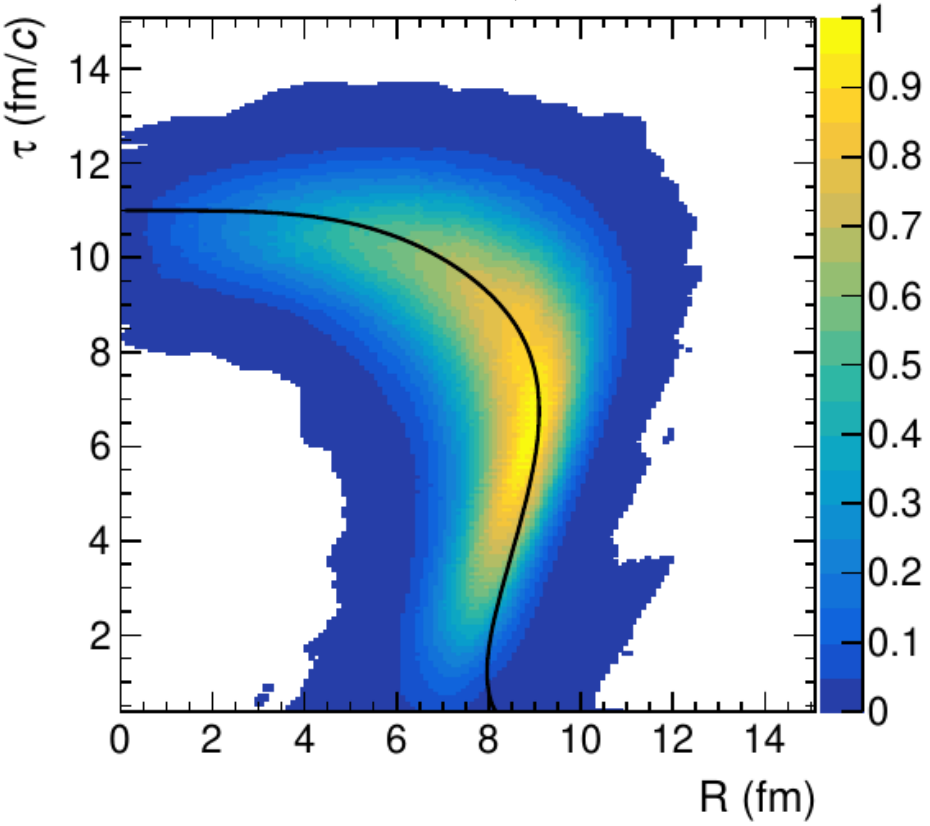

freeze-out hyper surface elements
at T=156.5 MeV from MUSIC
solid line: FluiduM

resulting J/ψ spectra including corona contribution and feed-down from B

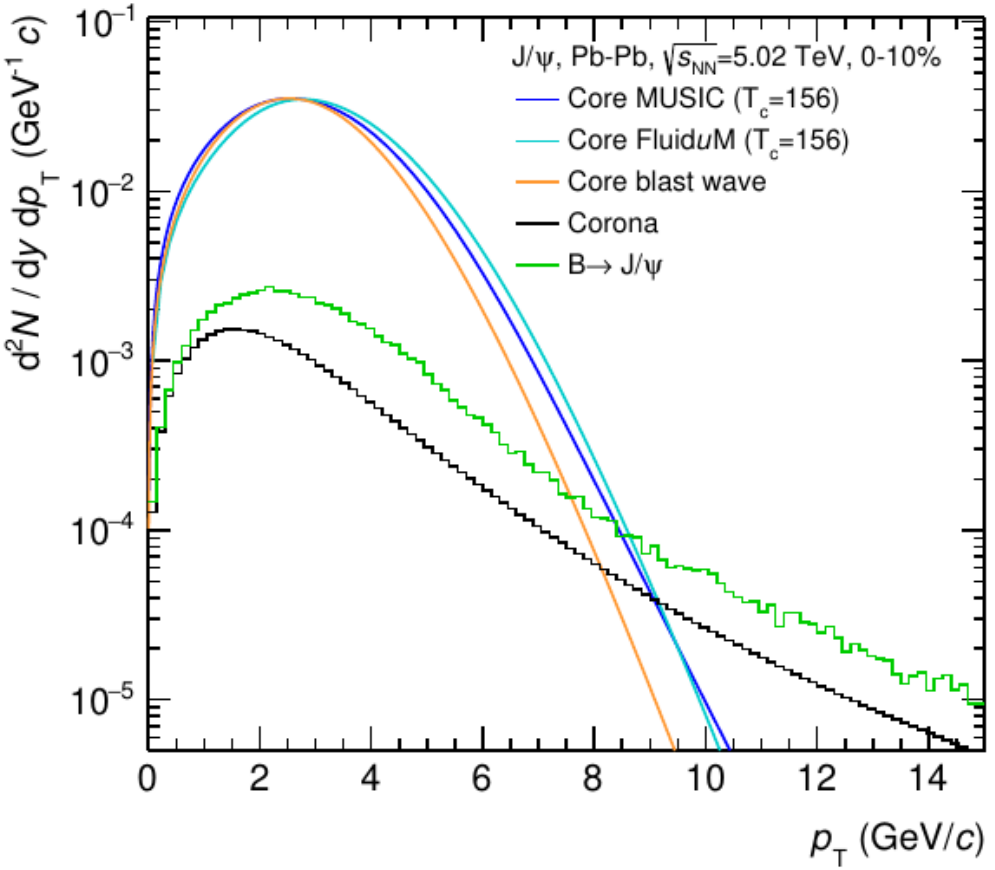

J/ψ transverse momentum spectra

A. Andronic, P. Braun-Munzinger, J. Brunßen, J. Crkovska, J. Stachel, V. Vislavicius, M. Völkl, arXiv: 2308.14821

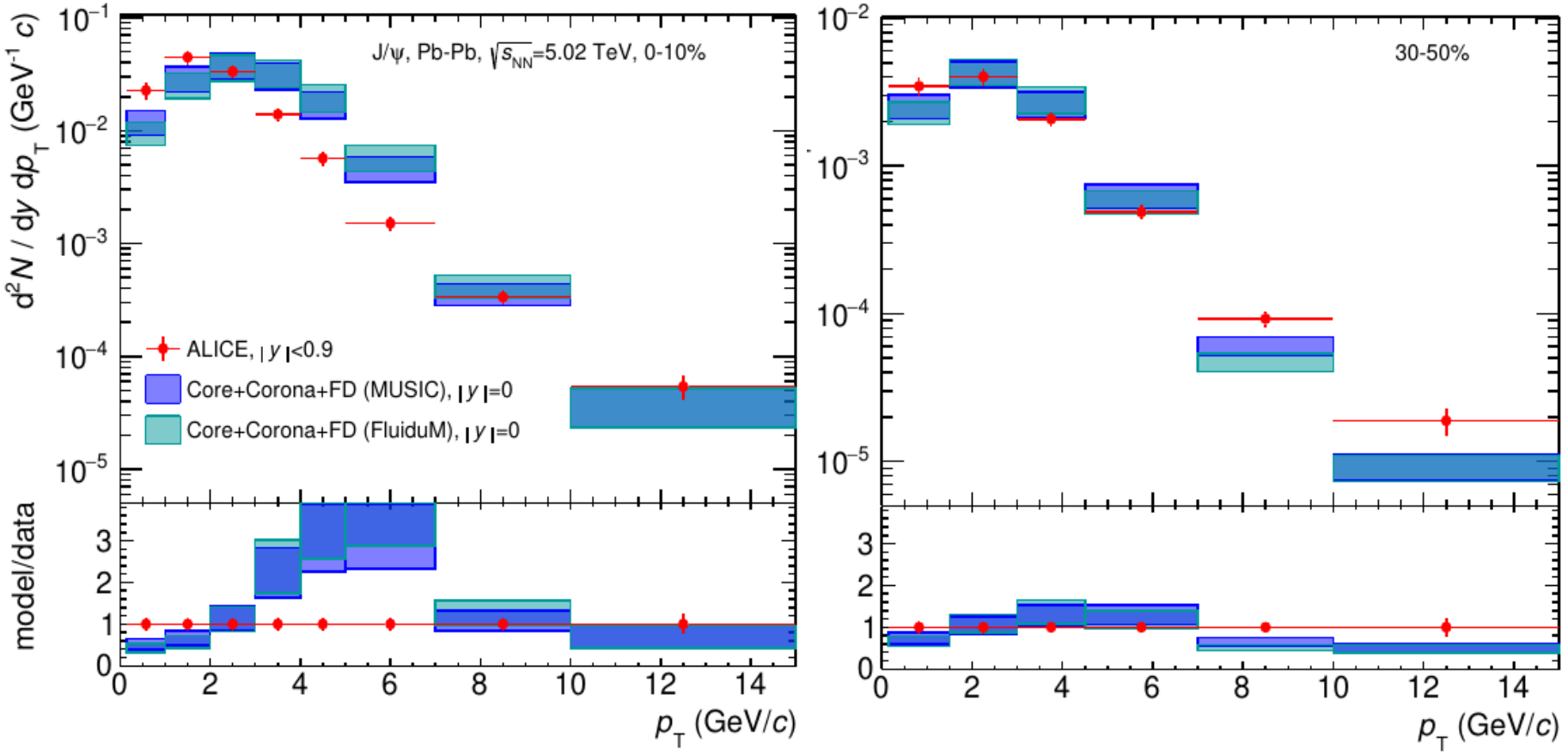

- for central collisions somewhat too much flow – shift by about 1 GeV
- are charm quarks reaching the very outer front of the expanding fireball?

Spectra of D mesons and Λ_c baryons

for open heavy flavor hadrons strong contribution from resonance decays
- include all known charm hadron states as of PDG2020 in SHMc
- compute decay spectra with FastReso: 76 2-body and 10 3-body decays

(A. Mazeliauskas, S. Floerchinger, E. Grossi, D. Teaney, EPJ C79 (2019) 284)

A.Andronic, P.Braun-Munzinger, M.Köhler, A.Mazeliauskas, K.Redlich, JS,V.Vislavicius JHEP 07 (2021) 035

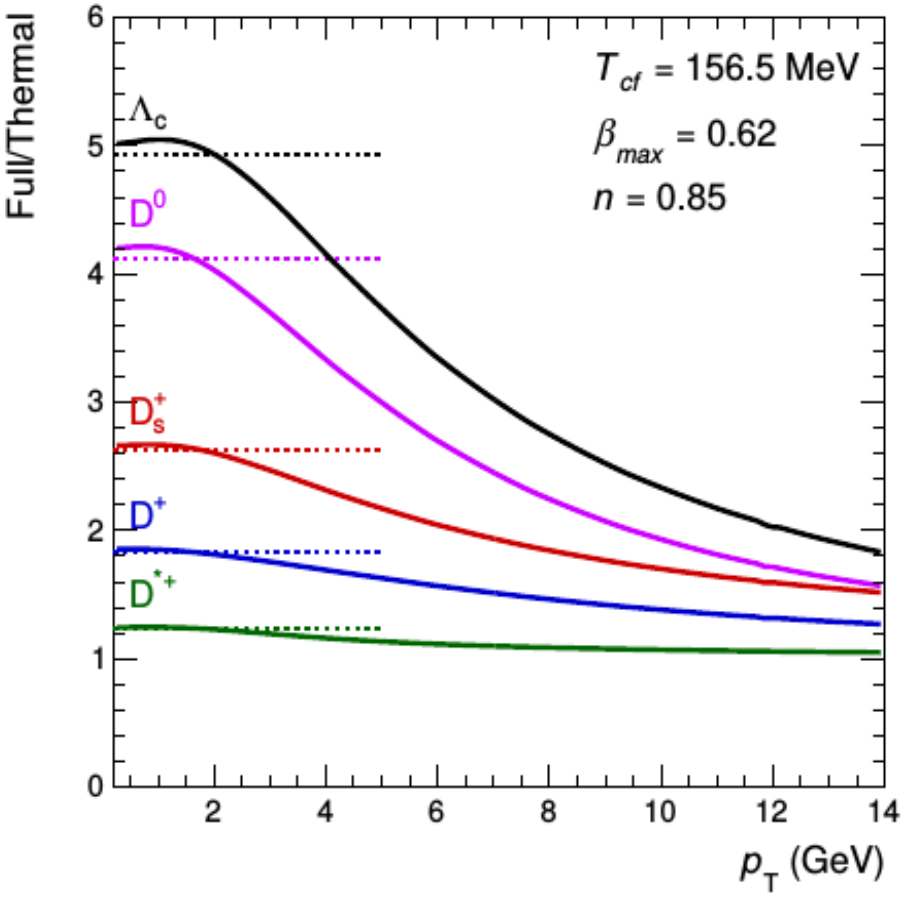

impact of resonance decays

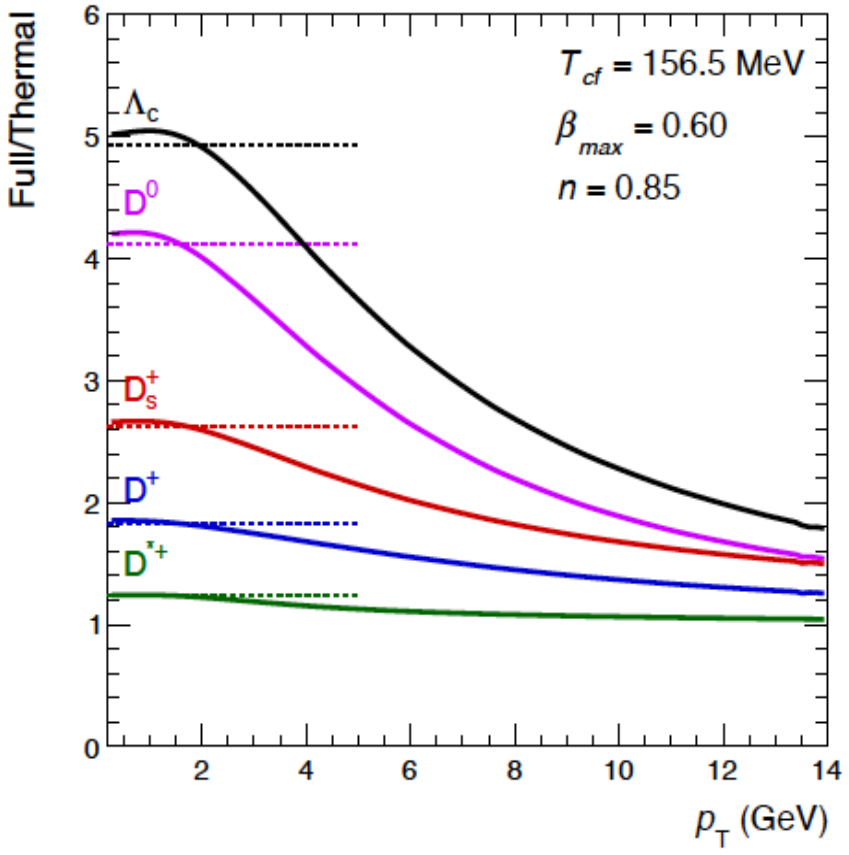

feed-down to Λc

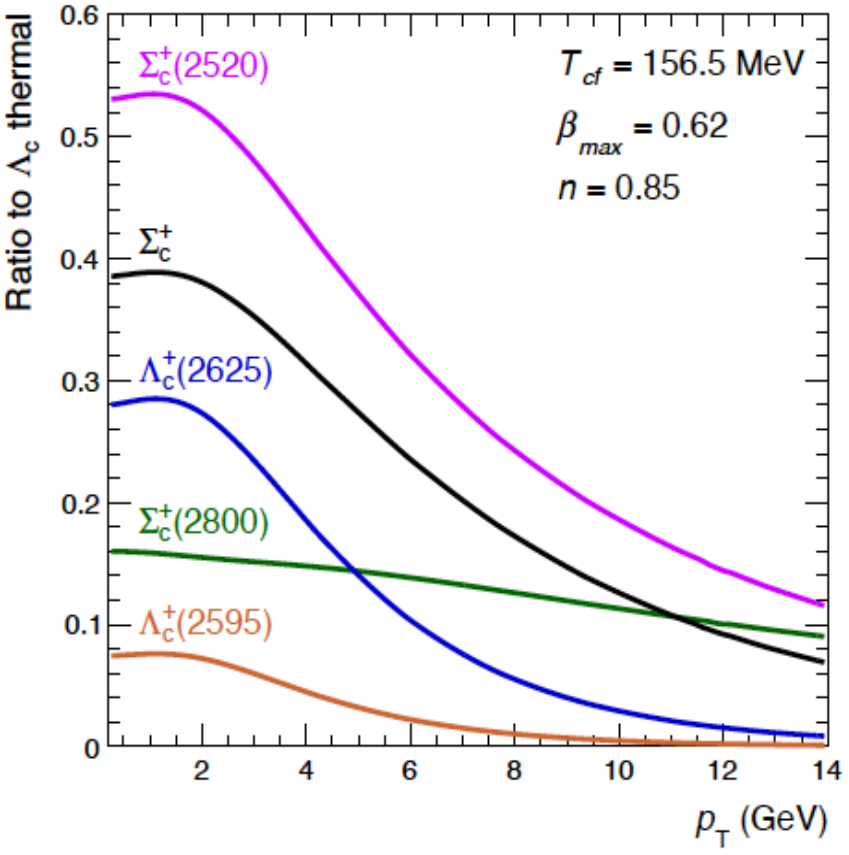

feeding very imporrant for D mesons and Λc baryons

transverse momentum spectrum for $\chi_{c1}(3872)$ in the SHMc

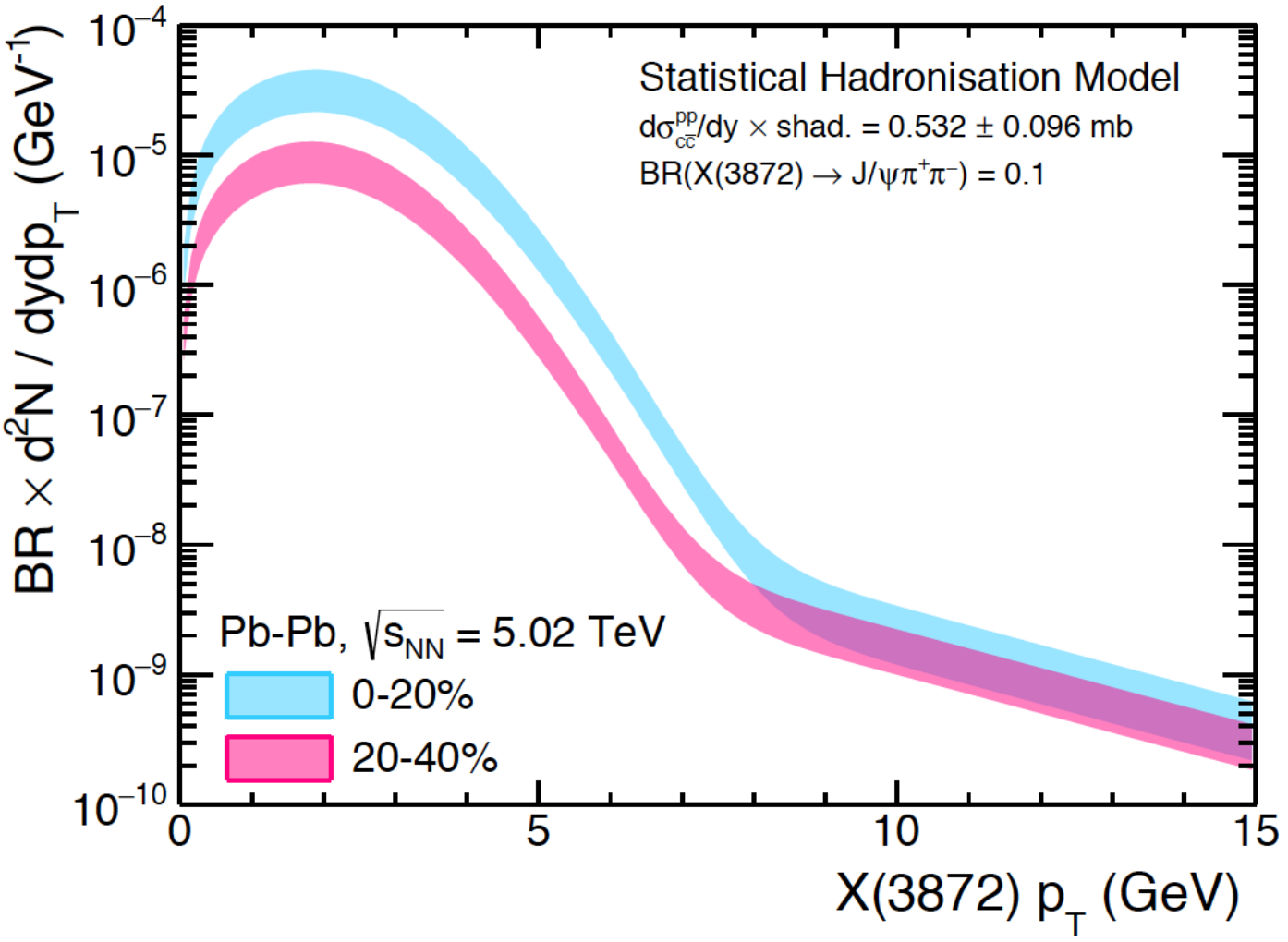

note: dramatic enhancement at low p_t predicted

Open charm spectra – examples D^0 and Λ_c

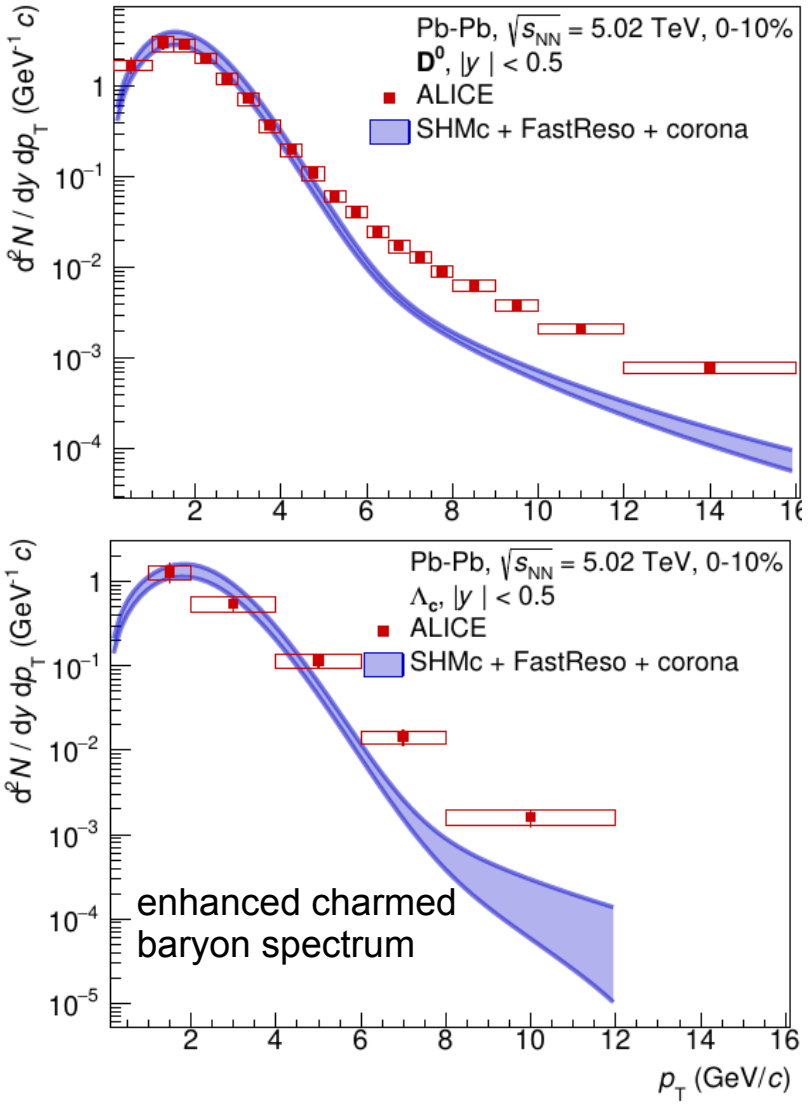

A. Andronic, P. Braun-Munzinger, J. Brunßen,
J. Crkovska, J. Stachel, V. Vislavicius, M. Völkl,
arXiv: 2308.14821

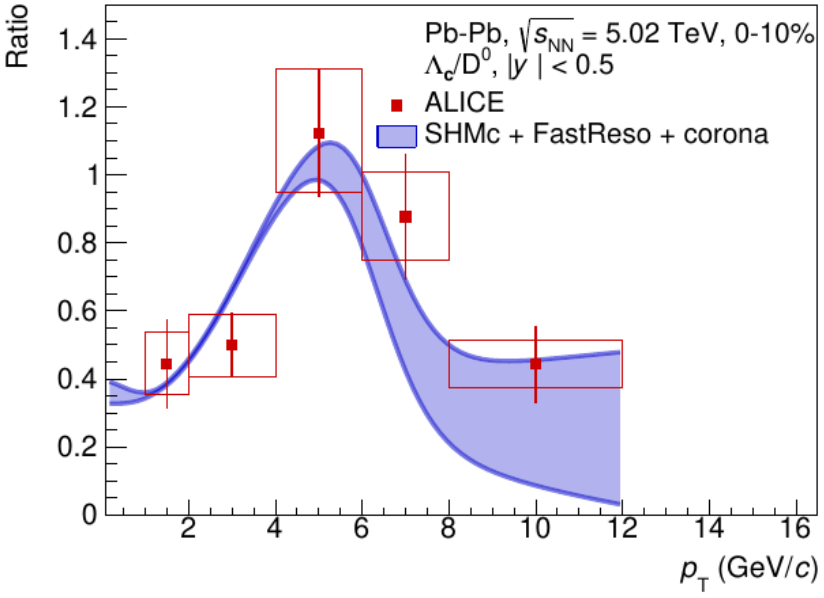

very good description of low and intermediate p_t data
maximum in ratio arises naturally from expansion

blast wave parametrization of transverse momentum spectrum

$$\frac{\mathrm{d}^2N}{2\pi p_{\mathrm{T}} dp_{\mathrm{T}} dy} = \frac{2J+1}{(2\pi)^3}\int \mathrm{d}\sigma_\mu p^\mu f(p)$$

$$= \frac{2J+1}{(2\pi)^3}\int_0^{r_{\max}} \mathrm{d}r\ \tau(r) r \left[K_1^{\mathrm{eq}}(p_{\mathrm{T}}, u^r) - \frac{\partial\tau}{\partial r} K_2^{\mathrm{eq}}(p_{\mathrm{T}}, u^r)\right]$$

$$K_1^{\mathrm{eq}}(p_{\mathrm{T}}, u^r) = 4\pi m_{\mathrm{T}} I_0\left(\frac{p_{\mathrm{T}} u^r}{T}\right) K_1\left(\frac{m_{\mathrm{T}} u^\tau}{T}\right)$$

$$K_2^{\mathrm{eq}}(p_{\mathrm{T}}, u^r) = 4\pi p_{\mathrm{T}} I_1\left(\frac{p_{\mathrm{T}} u^r}{T}\right) K_0\left(\frac{m_{\mathrm{T}} u^\tau}{T}\right)$$

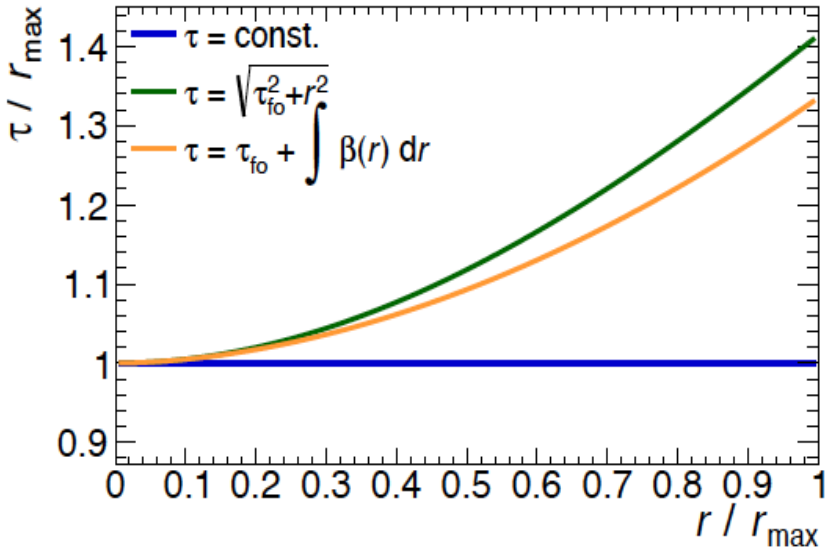

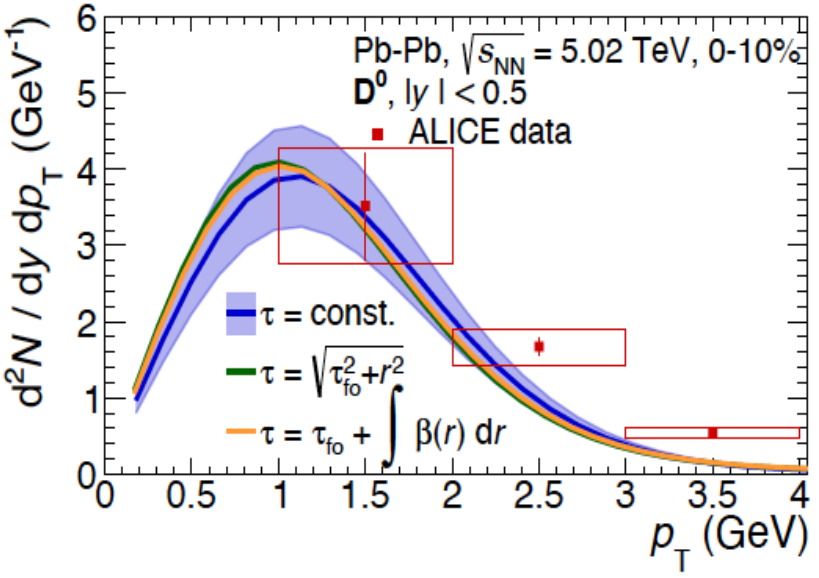

ALICE 3 – a nearly massless collider detector

inner tracker: curved Si, thickness: 0.1% RL
for LHC Run 5 and 6 (2034+)
Solenoid: 2T field
forward conversion tracker (FCT): for ultra-soft photons

→ Tracking precision $\times 4$: 4 μm at p_T = 1 GeV/*c*, "ultimate" Si-MAPS tracker
→ Acceptance $\times 4.5$: $|\eta| < 4$, $p_T > 50$ MeV, with particle ID (Si-TOF, SiPM-RICH, Mu)
→ Interaction rate $\times 5$ (pp $\times 25$)

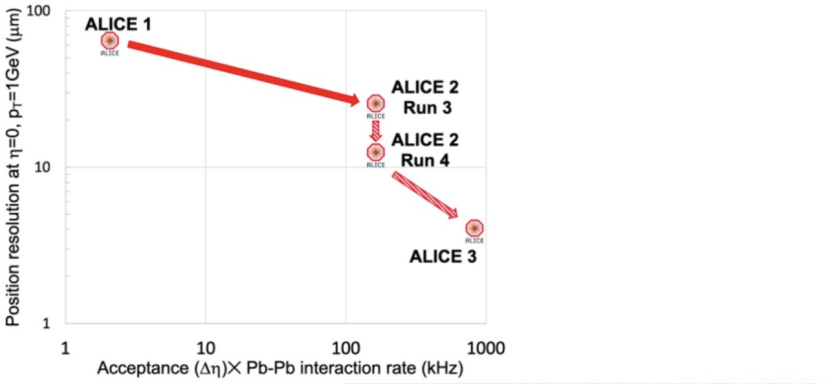

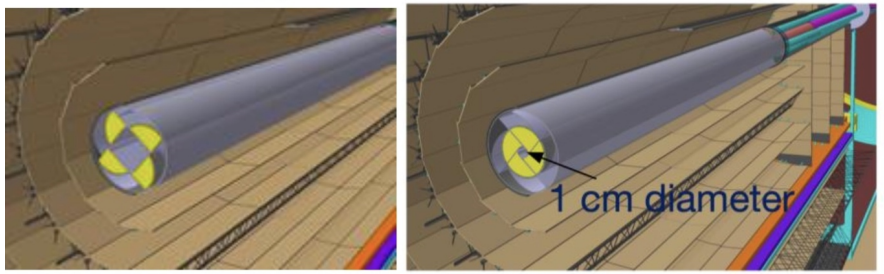

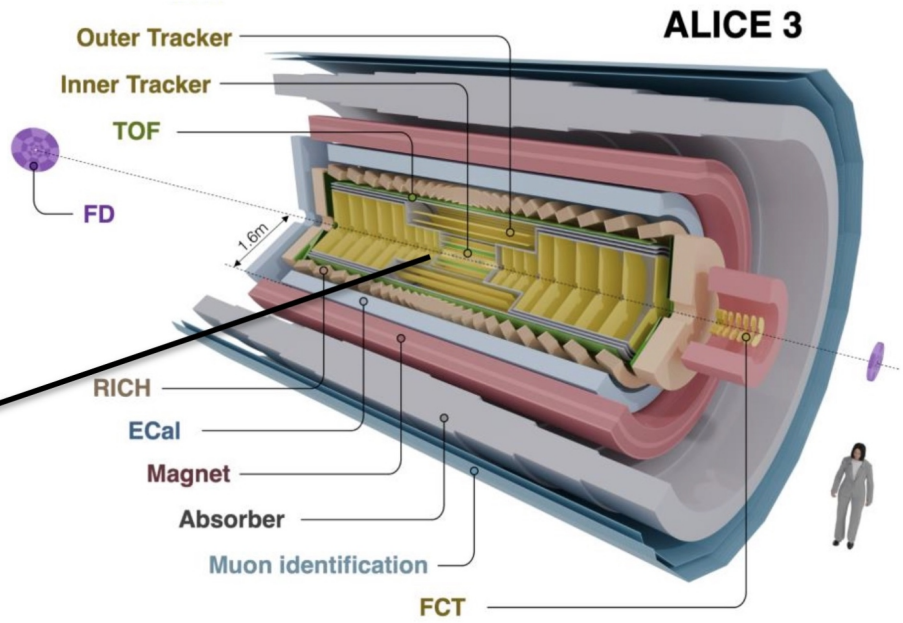

Letter of Intent: CERN-LHCC-2022-009
Scoping Document: CERN-LHCC-2025-002

ALICE 3

Outer and Middle Layers

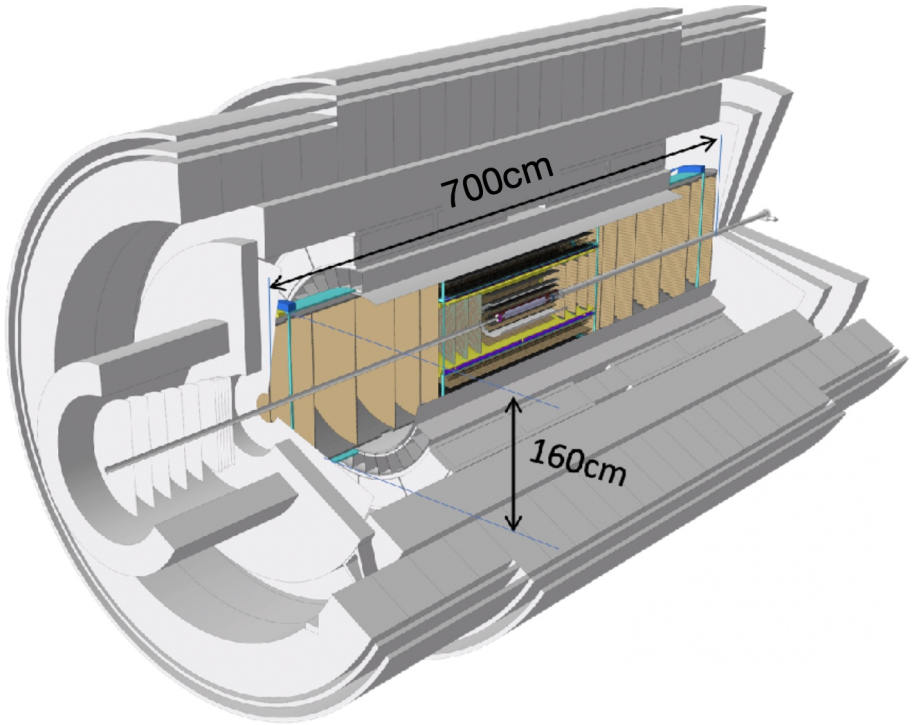

- **60 m²** silicon pixel detector
  - large coverage: ±4η
  - high-spatial resolution: ≈ 10 μm
  - very low material budget: X/X_0 (total) ≲ 10%
  - time resolution: 100 ns
  - low power: ≈ 20 mW/cm²
- **Main R&D challenge**: its size
  - power consumption and distribution (both ways) are critical
  - module design for industrial production is necessary
- Relies on maturity, reliability and availability of a large quantity of MAPS
  - largely leverages from ITS2 and ITS3

important role of German groups in the preparation of ALICE 3 and outer tracker:
project leader of outer tracker: Laura Fabbietti, TUM
Kai Schweda, GSI : ALICE spokesperson (from Jan. 2026)
Bernhard Ketzer, Bonn, Harry Appelshaeuser + Henner Buesching + Alberica Toia, Frankfurt, Silvia Masciocchi + Ralf Averbeck, GSI, Johanna Stachel,+ Klaus Reygers, Heidelberg, Anton Andronic, Muenster

ALICE 3

Vertex Detector

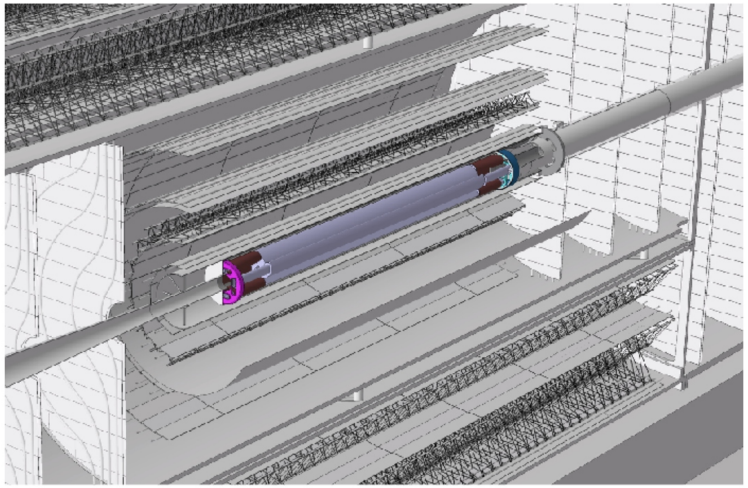

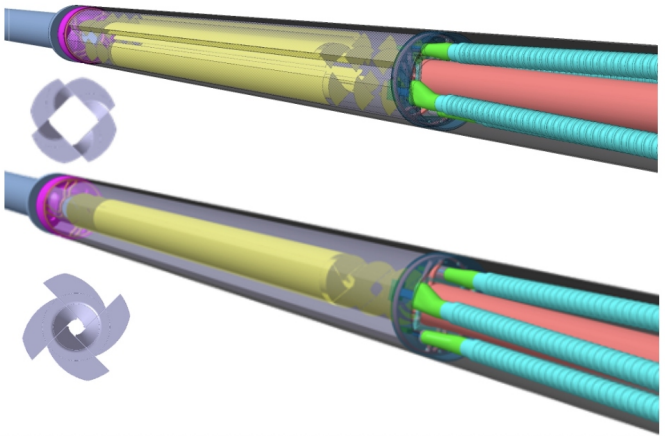

- **Based on wafer-scale, ultra-thin, curved MAPS**
  - radial distance from interaction point: 5 mm (inside beampipe, retractable configuration)
  - unprecedented spatial resolution: ≈ 2.5 μm
  - … and material budget: ≈ 0.1% X_0/layer
  - at radiation levels of: ≈ 10^{16} 1MeV n_{eq}/cm^2 + 300 Mrad
  - and hit rates up to: 94 MHz/cm^2
- Unprecedented performance figures
  - largely leverages on the ITS3 developments
  - pushes the technology on a number of fronts
- **R&D has started**

mid-rapidity yields for Pb-Pb collisions

Particle	dN/dy core (SHMc)	dN/dy corona	dN/dy total
		0-10%	
D^0	6.02 ± 1.07	0.396 ± 0.032	6.42 ± 1.07
D^+	2.67 ± 0.47	0.175 ± 0.026	2.84 ± 0.47
D^{*+}	2.36 ± 0.42	$0.160\ ^{+0.048}_{-0.022}$	2.52 ± 0.42
D_s^+	2.15 ± 0.38	$0.074\ ^{+0.024}_{-0.015}$	2.22 ± 0.38
Λ_c^+	1.30 ± 0.23	0.250 ± 0.028	1.55 ± 0.23
Ξ_c^0	0.263 ± 0.047	0.090 ± 0.035	0.353 ± 0.058
J/ψ	$0.108\ ^{+0.041}_{-0.035}$	$(5.08 \pm 0.37) \cdot 10^{-3}$	$0.113\ ^{+0.041}_{-0.035}$
$\psi(2S)$	$(3.04\ ^{+1.2}_{-1.0}) \cdot 10^{-3}$	$(7.61 \pm 0.55) \cdot 10^{-4}$	$(3.80\ ^{+1.2}_{-1.0}) \cdot 10^{-3}$
		30-50%	
D^0	0.857 ± 0.153	0.207 ± 0.017	1.06 ± 0.154
D^+	0.379 ± 0.068	0.092 ± 0.014	0.471 ± 0.069
D^{*+}	0.335 ± 0.060	$0.084\ ^{+0.025}_{-0.011}$	$0.419\ ^{+0.065}_{-0.061}$
D_s^+	0.306 ± 0.055	$0.039\ ^{+0.013}_{-0.008}$	0.344 ± 0.056
Λ_c^+	0.185 ± 0.033	0.131 ± 0.015	0.316 ± 0.036
Ξ_c^0	0.038 ± 0.007	0.047 ± 0.018	0.084 ± 0.020
J/ψ	$(1.12\ ^{+0.37}_{-0.32}) \cdot 10^{-2}$	$(2.65 \pm 0.19) \cdot 10^{-3}$	$(1.39\ ^{+0.37}_{-0.32}) \cdot 10^{-2}$
$\psi(2S)$	$(3.16\ ^{+1.04}_{-0.89}) \cdot 10^{-4}$	$(3.98 \pm 0.29) \cdot 10^{-4}$	$(7.14\ ^{+1.08}_{-0.94}) \cdot 10^{-4}$

dependence of Ω_{ccc} production yields on system size for a run time of 10^6 s

	O-O	Ar-Ar	Kr-Kr	Xe-Xe	Pb-Pb
$\sigma_{\mathrm{inel}}(10\%)\,\mathrm{mb}$	140	260	420	580	800
$T_{\mathrm{AA}}(0-10\%)\,\mathrm{mb}^{-1}$	0.63	2.36	6.80	13.0	24.3
$\mathcal{L}(\mathrm{cm}^{-2}\mathrm{s}^{-1})$	$4.5\cdot10^{31}$	$2.4\cdot10^{30}$	$1.7\cdot10^{29}$	$3.0\cdot10^{28}$	$3.8\cdot10^{27}$
	$\mathrm{d}\sigma_{\mathrm{c\bar{c}}}/\mathrm{d}y = 0.53\,\mathrm{mb}$				
$\mathrm{d}N_{\Omega_{ccc}}/\mathrm{d}y$	$8.38\cdot10^{-8}$	$1.29\cdot10^{-6}$	$1.23\cdot10^{-5}$	$4.17\cdot10^{-5}$	$1.25\cdot10^{-4}$
Ω_{ccc} Yield	$5.3\cdot10^{5}$	$8.05\cdot10^{5}$	$8.78\cdot10^{5}$	$7.26\cdot10^{5}$	$3.80\cdot10^{5}$
	$\mathrm{d}\sigma_{\mathrm{c\bar{c}}}/\mathrm{d}y = 0.63\,\mathrm{mb}$				
$\mathrm{d}N_{\Omega_{ccc}}/\mathrm{d}y$	$1.44\cdot10^{-7}$	$2.33\cdot10^{-6}$	$2.14\cdot10^{-5}$	$7.03\cdot10^{-5}$	$2.07\cdot10^{-4}$
Ω_{ccc} Yield	$9.2\cdot10^{5}$	$1.45\cdot10^{6}$	$1.53\cdot10^{6}$	$1.22\cdot10^{6}$	$6.29\cdot10^{5}$

example: chi_c1(3872)

X(3872)

- 2003 -

$$B^{\pm} \to K^{\pm}\pi^{+}\pi^{-}J/\psi$$

$$M = 3872.0 \pm 0.6 \pm 0.5\ \text{MeV}$$

- 2013 -

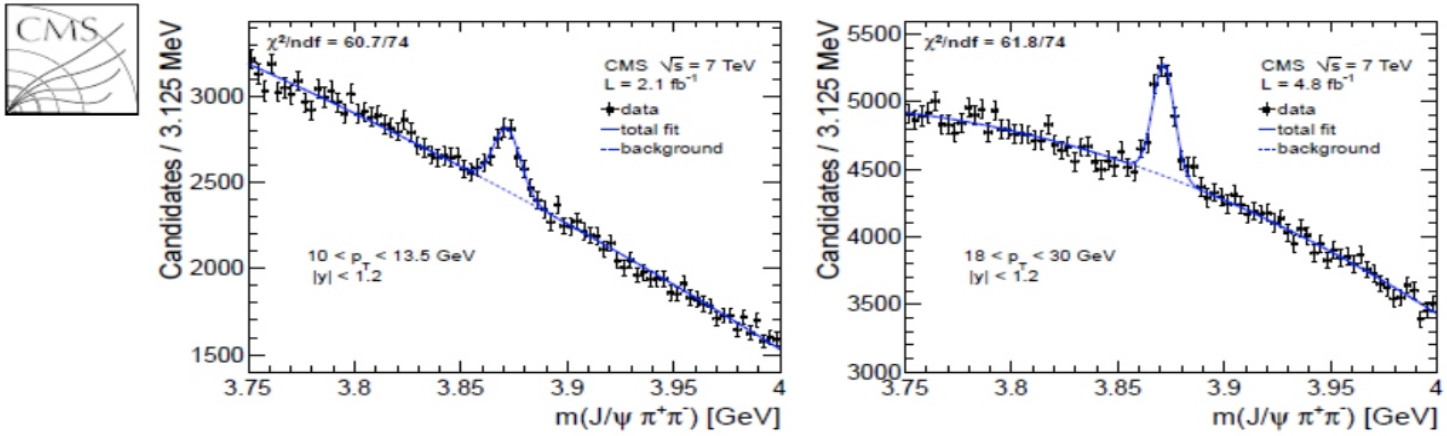

PDG particle data group

X(3872)

$$I^G(J^{PC}) = 0^+(1^{++})$$

Mass $m = 3871.69 \pm 0.17$ MeV

$m_{X(3872)} - m_{J/\psi} = 775 \pm 4$ MeV

$m_{X(3872)} - m_{\psi(2S)}$

Full width $\Gamma < 1.2$ MeV, CL = 90%

22

J/psi and hyper-triton described with the same flow parameters in the statistical hadronization model

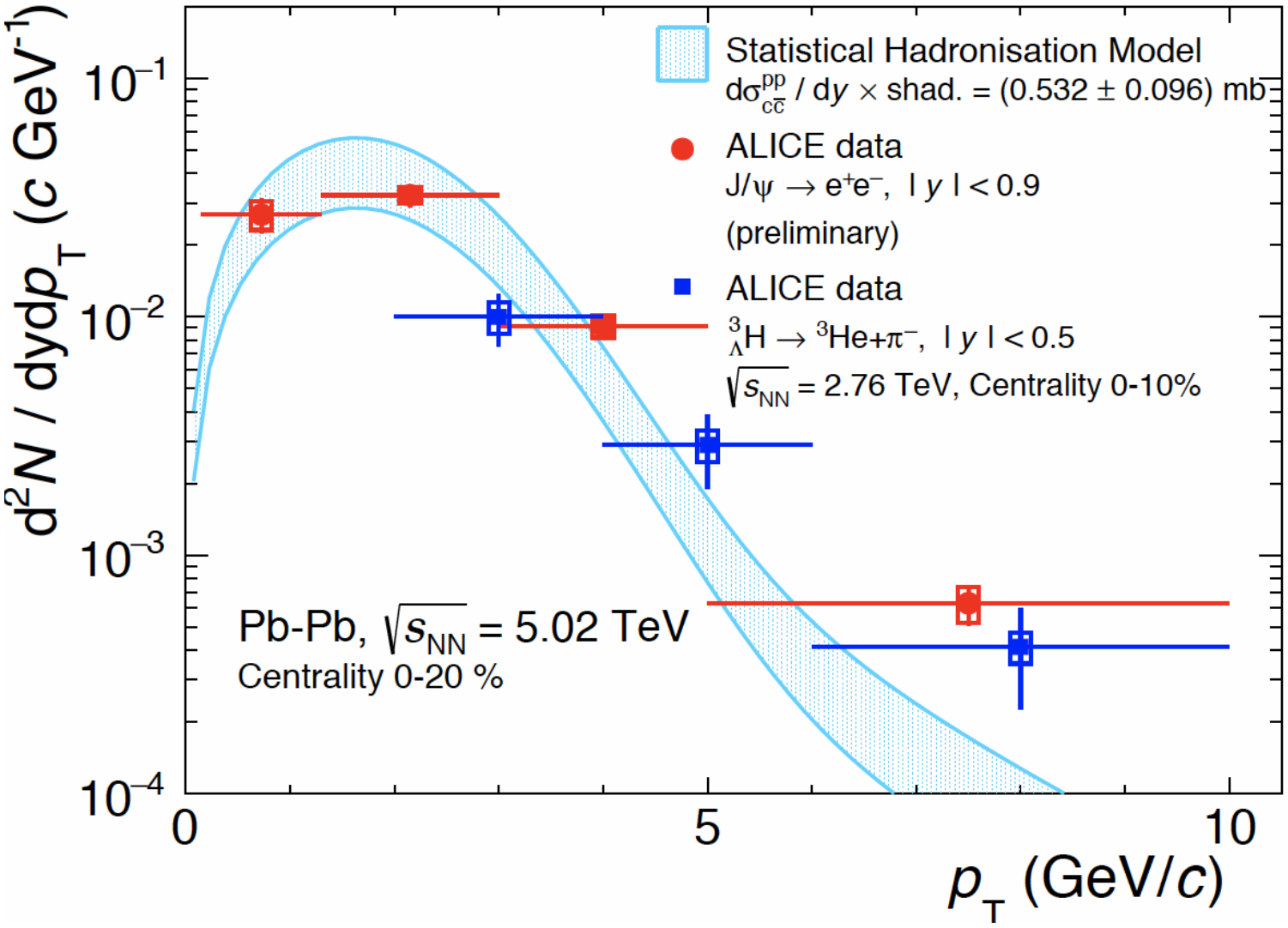

binding energies:
J/psi 600 MeV
hypertriton 2.2 MeV
Lambda S.E. 0.2 MeV

from review: hypernuclei and other loosely bound objects produced in nuclear collisions at the LHC,
pbm and Benjamin Doenigus,
Nucl. Phys. A987 (2019) 144, arXiv:1809.04681

charmonium at LHC: peaks at mid-y and strong enhancement at low transverse momentum

nuclear modification factor: $R_{\mathrm{AA}}(p_{\mathrm{T}}) = \dfrac{\mathrm{d}N^{\mathrm{AA}}/\mathrm{d}p_{\mathrm{T}}}{\langle N_{\mathrm{coll}}\rangle \mathrm{d}N^{\mathrm{PP}}/\mathrm{d}p_{\mathrm{T}}}$

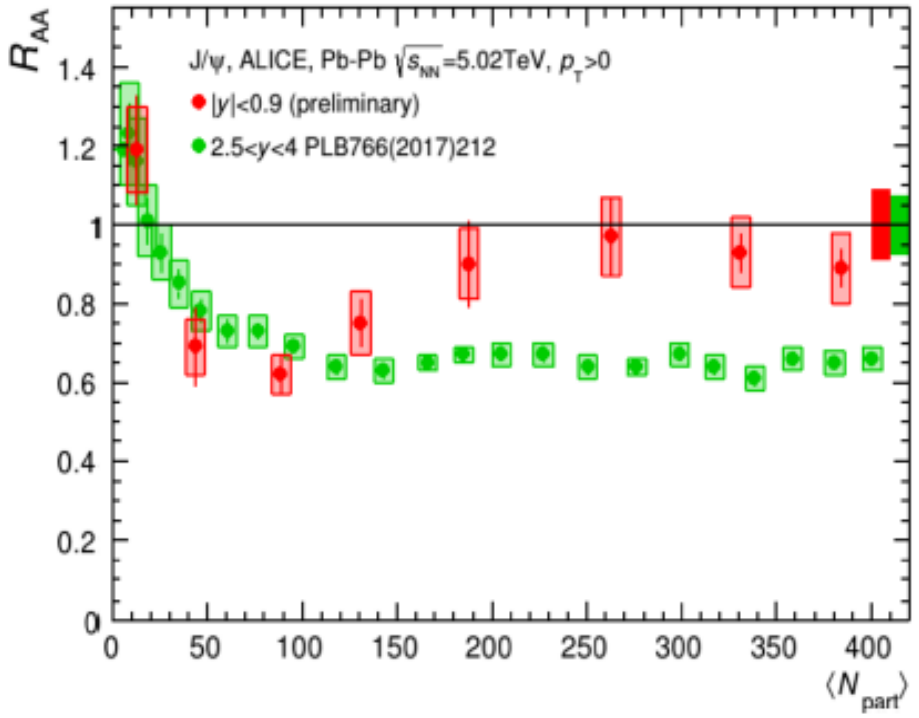

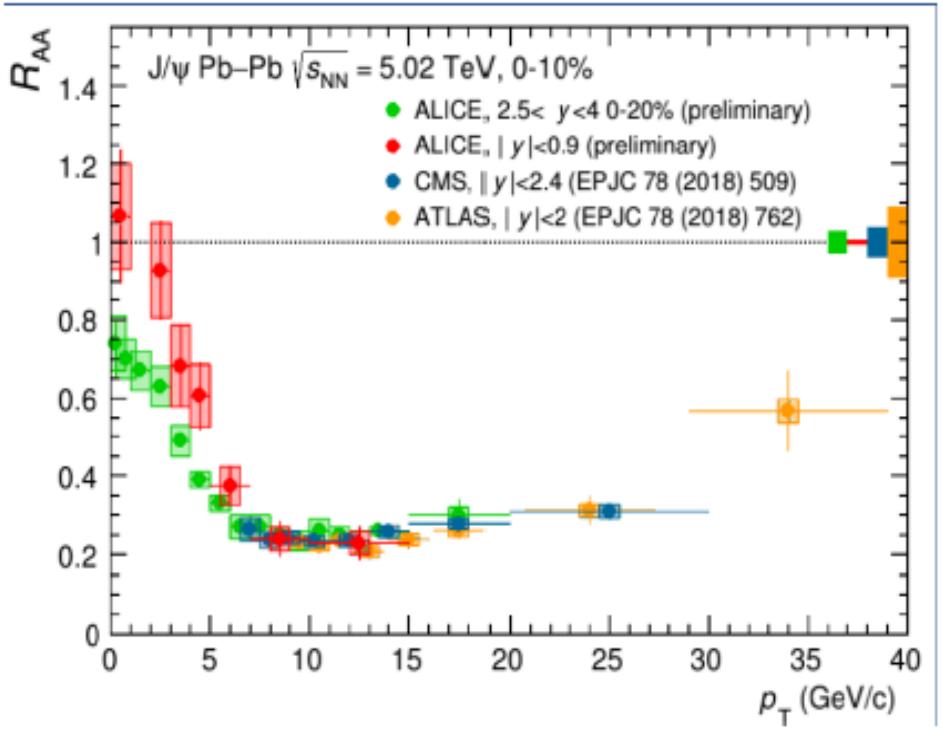

RHIC and LHC data compared to SHMc predictions

note the energy dependence of the nuclear modification factor R_{AA}

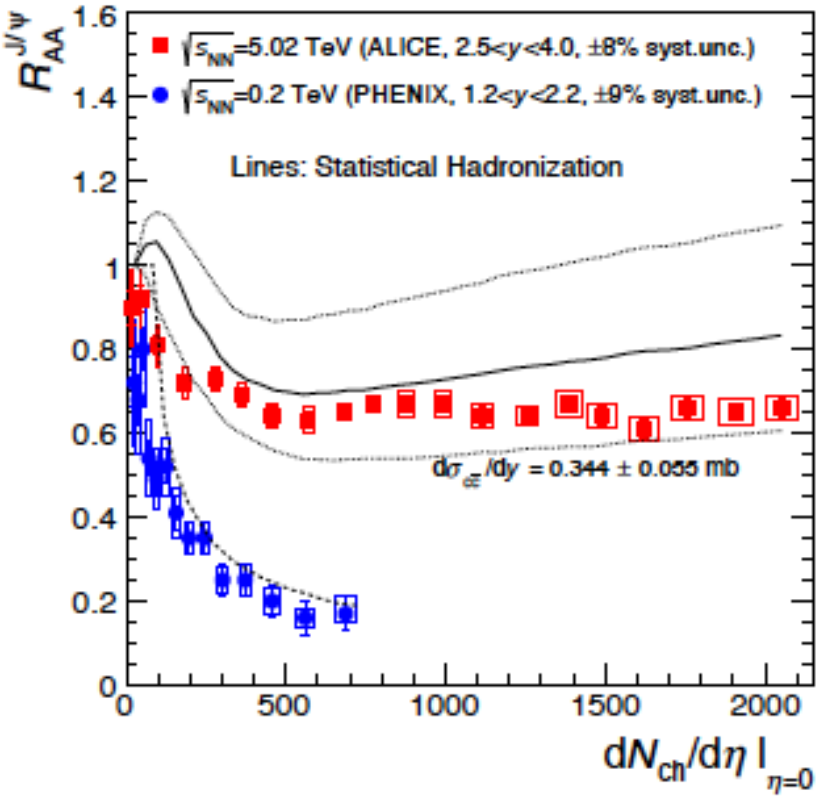

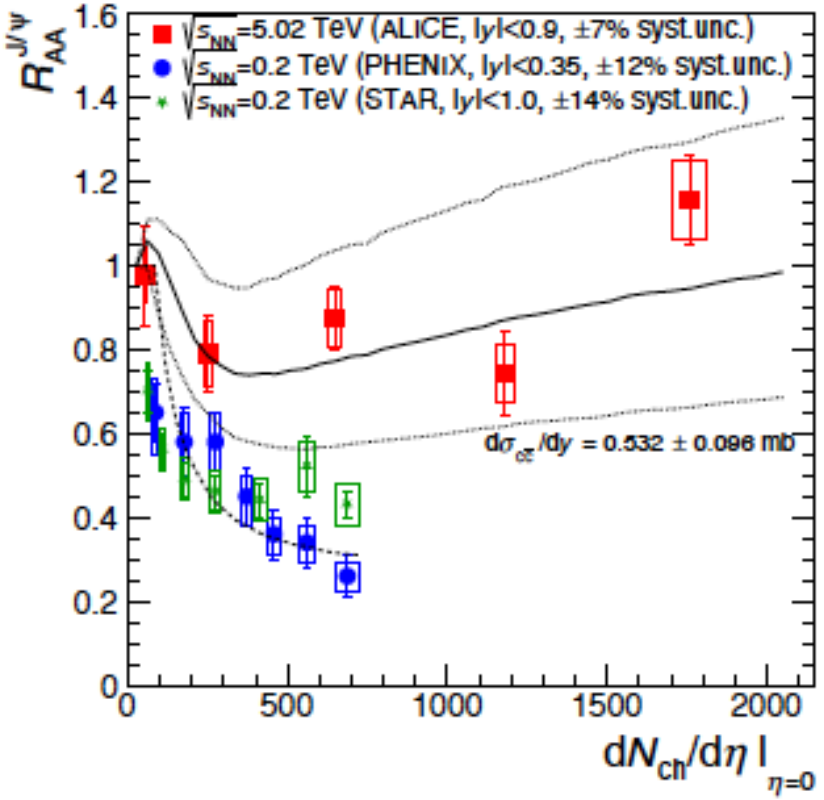

the band with the model predictions at LHC energy is due to the uncertainties in the pp open charm cross section and the necessary shadowing corrections

beyond yields: transverse momentum distributions

assume thermalization of charm quarks in QGP, charm quarks follow collective flow
use hydro velocity profile at pseudocritical temperature from MUSIC (3+1) D
tuned to light flavor observables

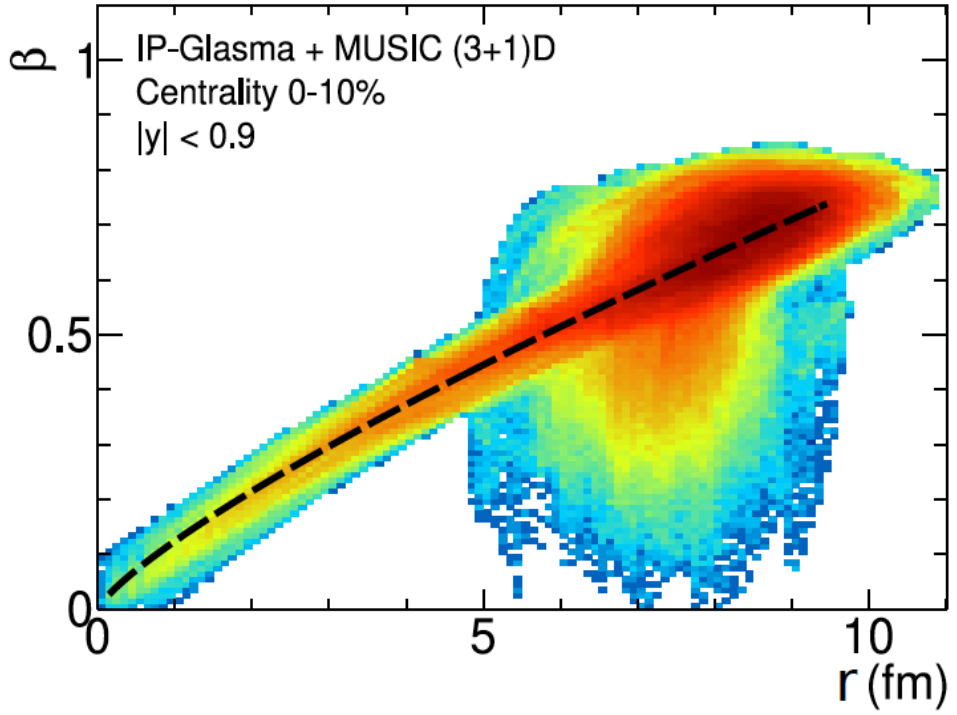

$$\beta(r) = \beta_{\max}\frac{r^n}{r^n_{\max}}$$

$$\beta_{\max} = 0.62$$

$$n = 0.85$$

$$V = 2\pi \int_0^{r_{\max}} \mathrm{d}r\; r\tau(r)u^\tau \left[1 - \beta(r)\frac{\partial\tau}{\partial r}\right]$$

$$V = 4997\,\mathrm{fm}^3$$

and blast wave parametrization of spectral shape with T = 156.5 MeV and
a fireball volume per unit rapidity for central PbPb collisions V = 4997 fm^3
sensitivity to shape of freeze-out surface: backup

charm fugacities and canonical suppression factors

different collision systems:

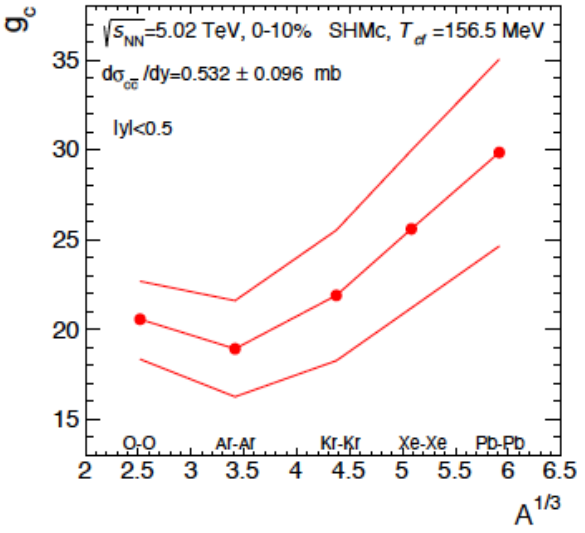

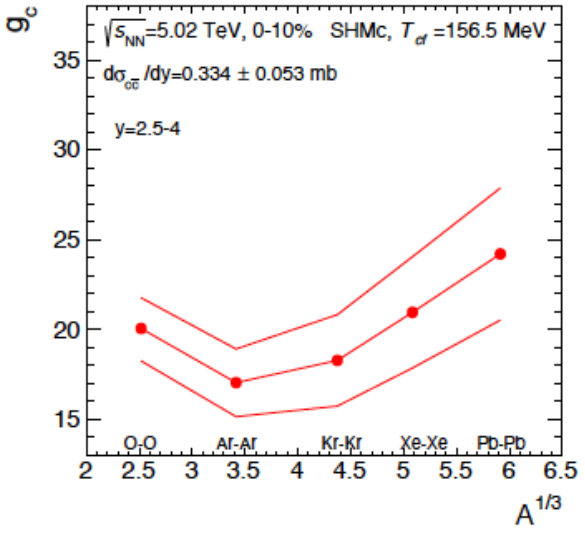

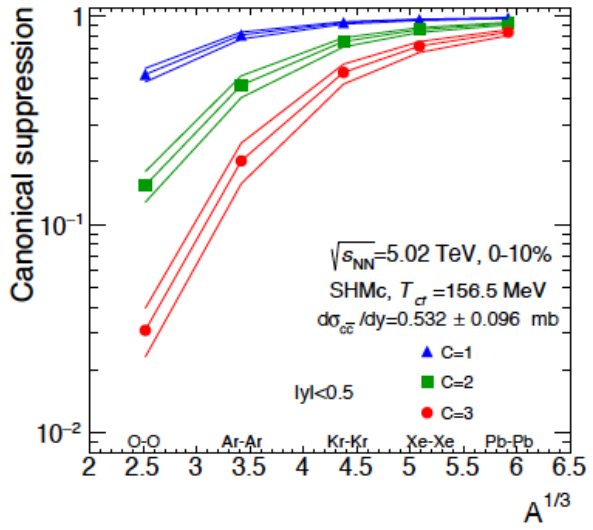

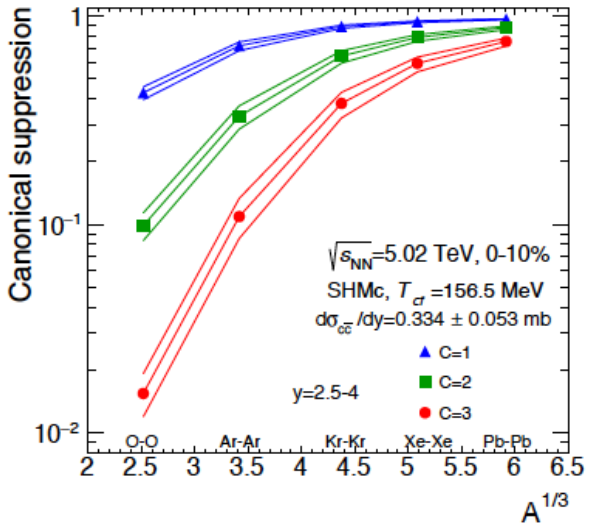

energy dependence of T and mu_B

Nucl. Phys. A 772 (2006) 167-199

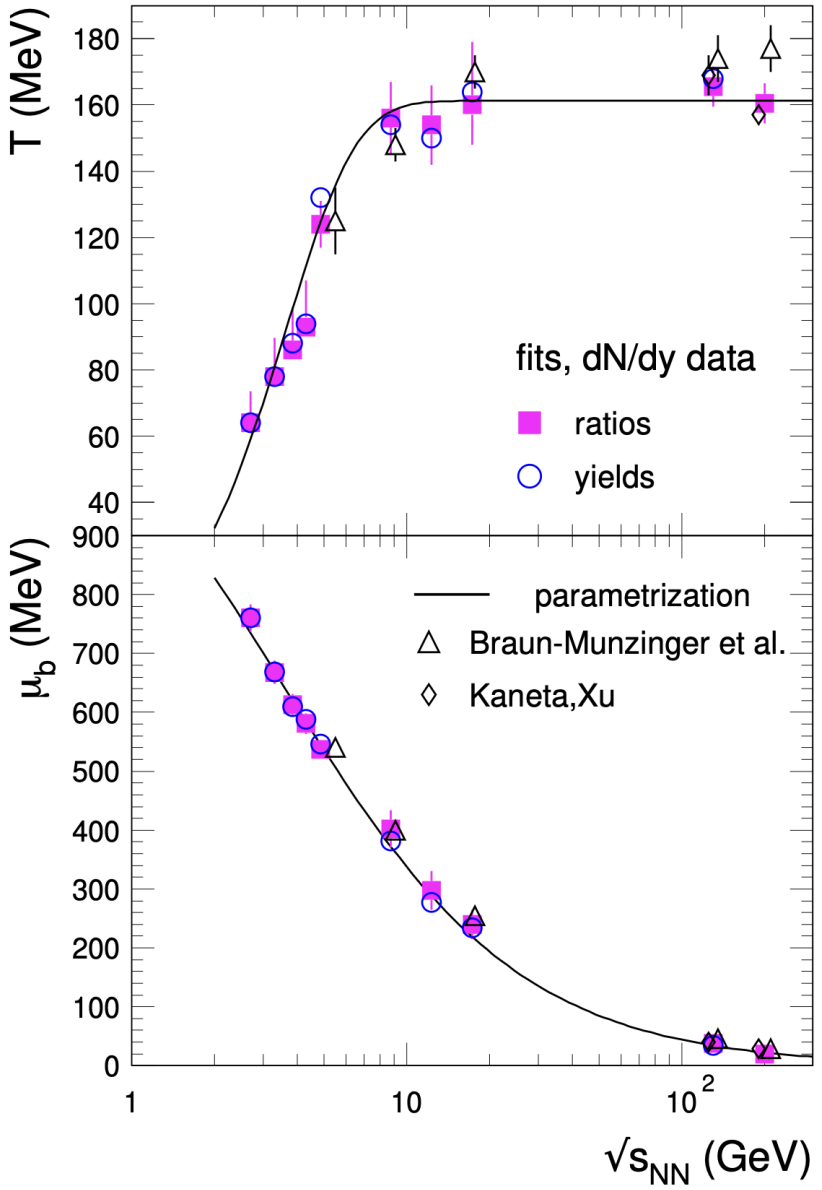

QCD phase diagram vs ‘slope of dilepton mass spectrum’

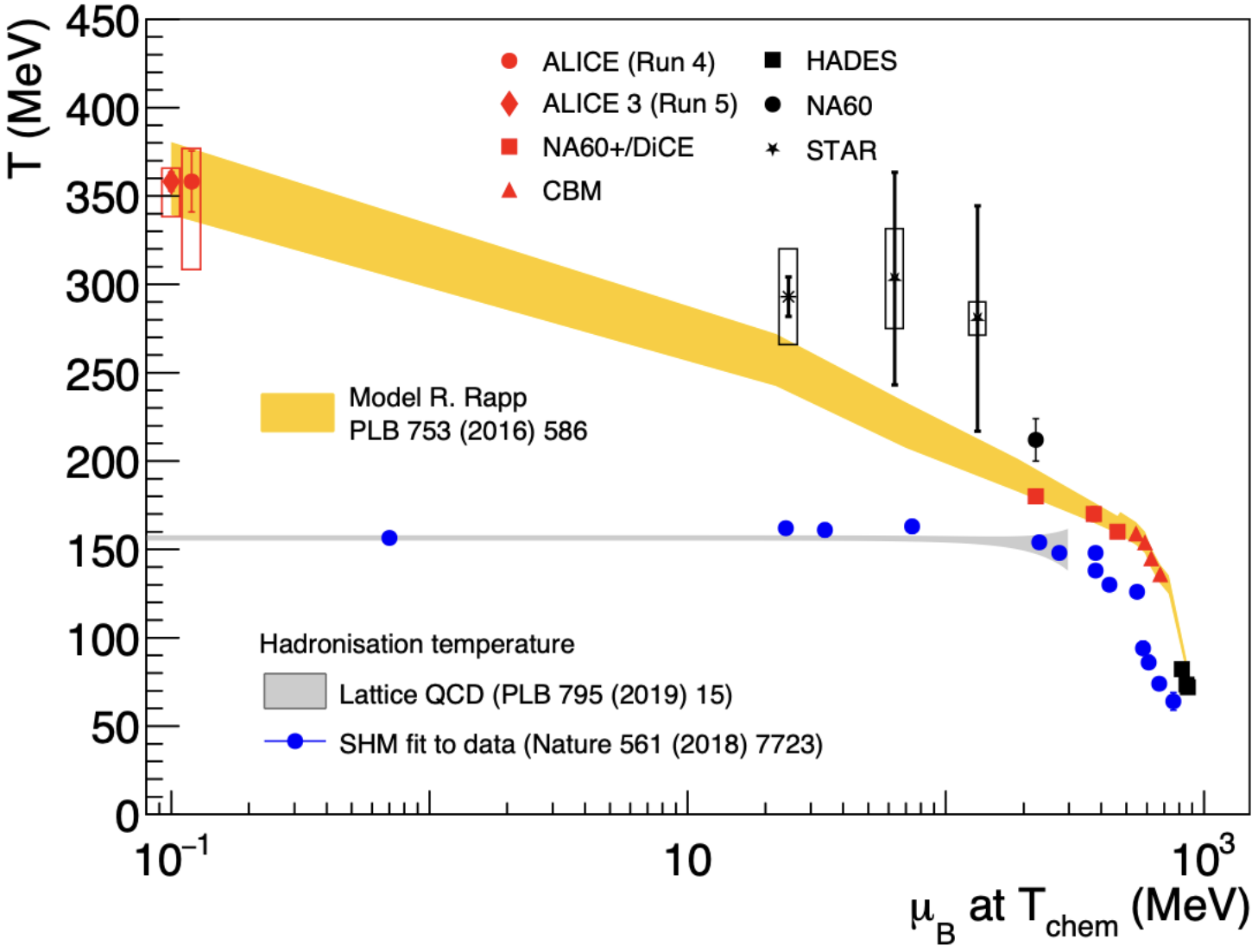

blue points result from analysis of mean particle multiplicities of > 10 different types for central Pb-Pb or Au-Au collisions at different collision energies (chemical freeze-out).

Unique prediction of SHMc – open charm/charmonium

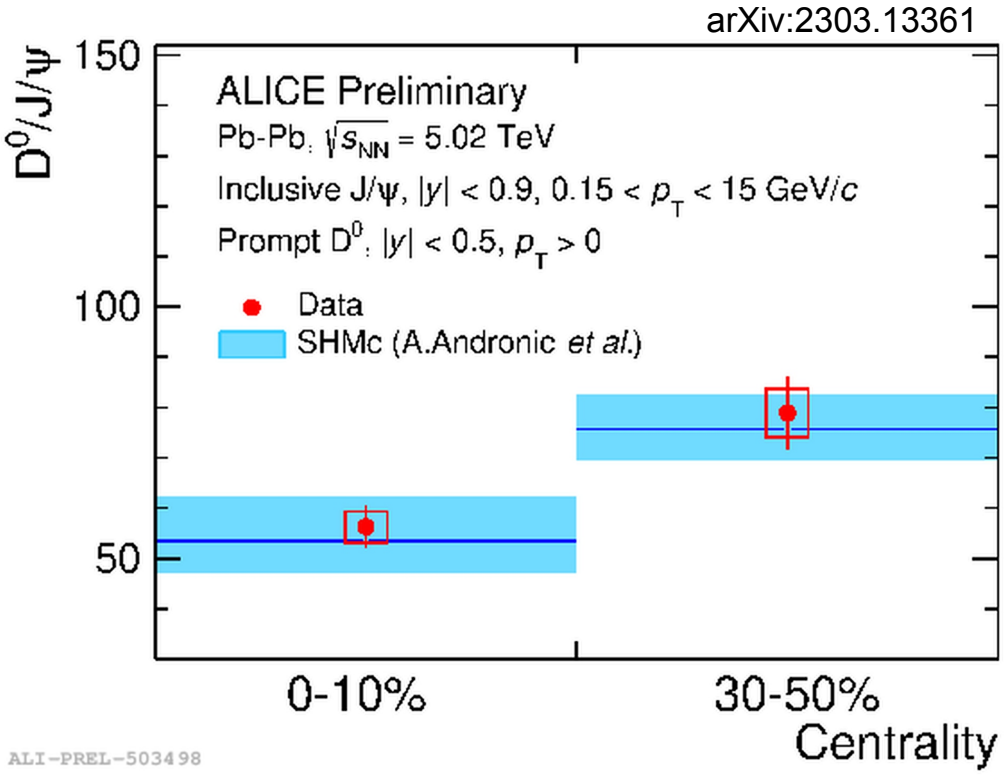

for the first time ratio of fully p_t integrated D^0 to J/ψ available from ALICE

D^0: cubar, m = 1.9 GeV, J=0
J/ψ: ccbar, m = 3.1 GeV, J = 1
in SHMc yield ratio governed by masses, degeneracy, strong feeding, and g_c

→ J/ψ relative to D^0 falls into place naturally, small uncertainties

QCD phase diagram from 'statistical hadronization model'

update 2025

hadronic matter cannot be heated to $T > T_{CF}$ even at LHC energy

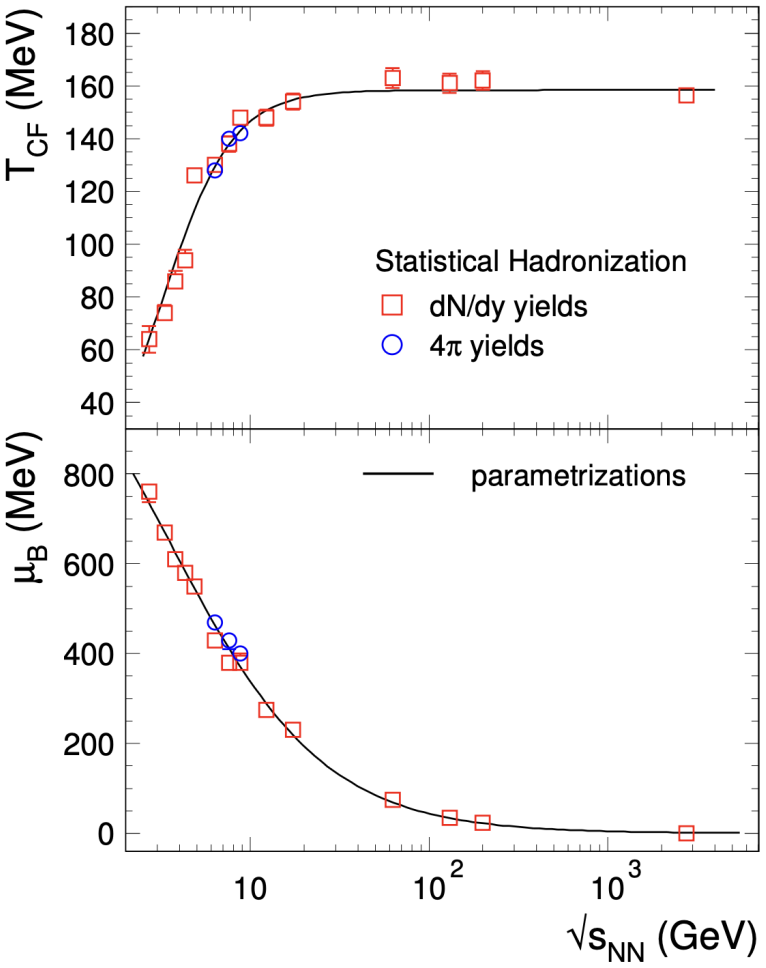

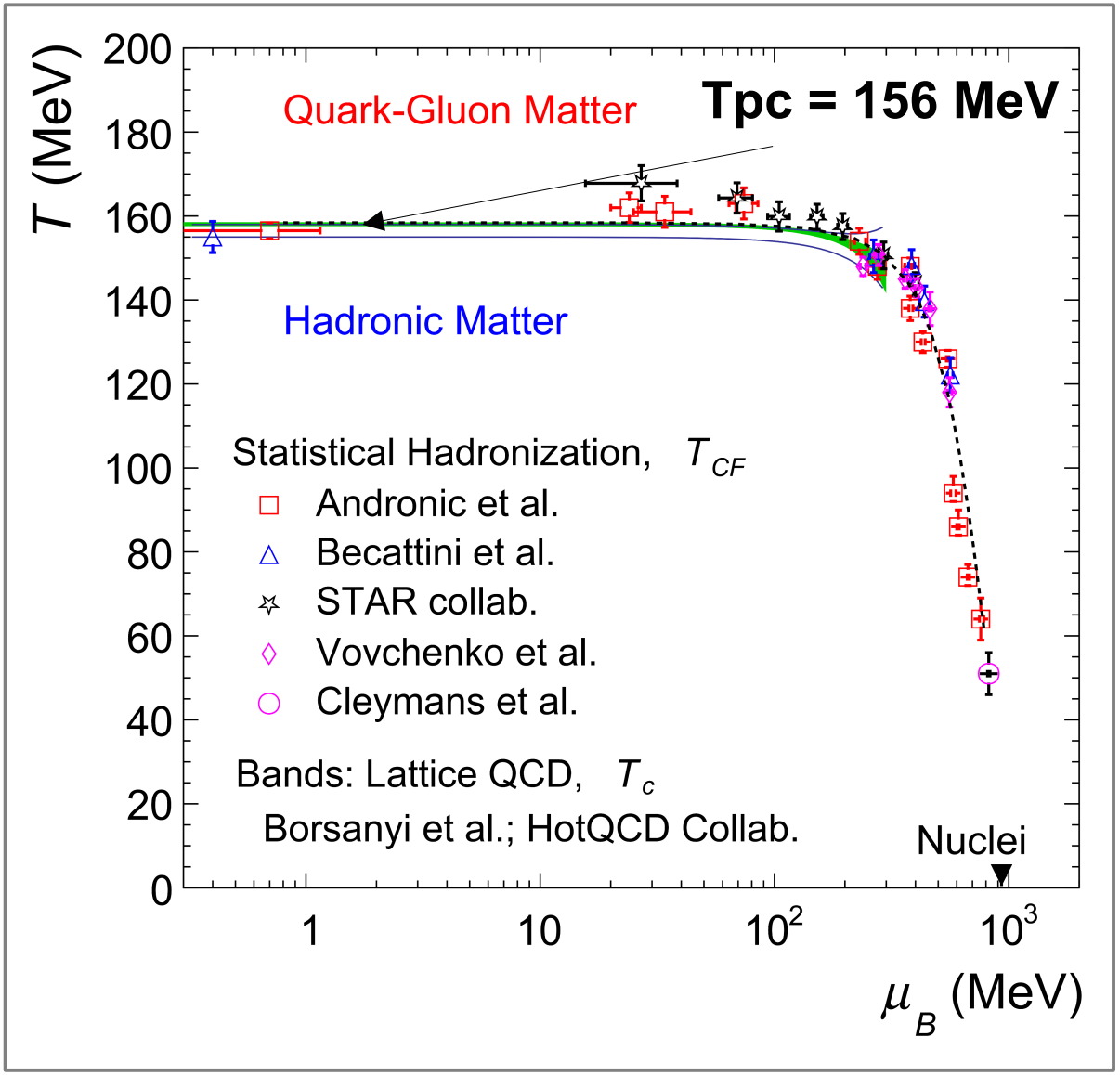

lattice predictions in quantitative agreement with results from statistical hadronization model

Conclusion of European Strategy Meeting, June 2025, Venice

slide: courtesy of Urs Wiedemann, CERN

Quantitative support for a default picture of AA

$\tau_{dec.} \approx 10$ fm/c
$V_{dec.} \approx 5000$ fm^3
$\varepsilon(\tau_{dec.}) \approx 0.4$ GeV/fm^3

$T_{kin.} \approx 100 - 150$ MeV
$v_{T,kin.} \approx 0.65\ c$
$\tau_{hadr.} \approx 1 -$ few fm/c

$T_{chem.} = 156 \pm 2$ MeV

η/s at $T_c \approx 0.06 - 0.12$
$2\pi T D_s$ at $T_c \approx 1.5 - 4.5$
$T_{photon} = 304 \pm 41$ MeV

$\varepsilon(1\ \text{fm}/c) \approx 14$ GeV/fm^3